Dealing with morphometric data in fossil vertebrates: a case-study of the intra-specific variation and allometry of the skull of Late Cretaceous side-necked turtle *Bauruemys elegans* (Pleurodira, Podocnemididae)

Thiago Fiorillo Mariani[1], Pedro Seyferth R. Romano[1]

[1] Departamento de Biologia Animal, Universidade Federal de Viçosa, Viçosa, Minas Gerais, Brazil.

Corresponding author:

Thiago Mariani[1]

Av. P. H. Rolfs, Anexo do Centro de Ciências Biológicas II, Third Floor, Room 305, Viçosa, Minas Gerais, 36570-900, Brazil

Email address: tmariani.bio@gmail.com

19

20

21 **1. Introduction**

22 **1.1. Principal Component Analysis and fossil sampling bias**

23 Paleontological data are intrinsically scarce (Strauss, Atanassov & Oliveira, 2003; Hammer &
24 Harper, 2006), leading to incomplete data sampling. This limitation impacts several approaches
25 inpaleontological studies, especially inter-specific variation analyses. Although there are some
26 approaches proposed to deal with missing entries in fossil datasets (e.g.: Norell & Wheeler,
27 2003; Strauss, Atanassov & Oliveira, 2003), sometimes the study relies on a statistic exploratory
28 evaluation of general structure in the data and Principal Component Analysis (PCA) is
29 commonly used for this purpose.

30 PCA is a multivariate and exploratory analysis. Its aim is to identify the variables that account
31 for the majority of the variance within a multivariate matrix, by means of linear combinations of
32 all variables, which are converted into components that are independent of each other (Strauss,
33 Atanassov & Oliveira, 2003; Hammer, Harper & Ryan, 2001). Hence, PCA summarizes a large
34 amount of the variance contained in the data (Krzanowski,1979; Hammer, Harper & Ryan,
35 2001). It thus reduces a multidimensional space into fewer components which retain the majority
36 of the variance of the sample (Jolicoeur & Mosimann, 1960; Peres-Neto, Jackson & Somers,
37 2003), and is therefore an useful tool for exploring large, complex data sets, being largely
38 applied to both extant and fossils vertebrates (e.g. Jolicoeur & Mosimann, 1960; Claude et al.,
39 2004; Depecker et al., 2005, 2006; Astua, 2009; Burnell, Collins & Young, 2012; Costa, Moura

& Feio, 2013; Bhullar et al., 2012; Fabre et al., 2014; Werneburg et al., 2014; Ferreira et al., 2015).

1.2. Case-study

1.2.1. Skull variation

The skull is one of the most variable structures in vertebrates because it concentrates several sensory organs, the brain, and the beginning of the respiratory and digestory systems, including chewing muscles (Smith, 1993). Consequently, the skull is the body portion with more phenotypes used in vertebrate cladistic analysis (Rieppel, 1993), as seen in turtles, in which most cladistic analysis rely mainly on cranial characters (e.g. Gaffney et al., 1991; de la Fuente, 2003; Gaffney et al., 2006, 2011; Joyce, 2007; Joyce & Lyson, 2010; Sterli et al., 2010; Sterli & de la Fuente, 2011a, b; Anquetin, 2012; Rabi et al., 2013; Romano et al., 2014; Ferreira et al., 2015;). Despite that, most of skull materials found in paleontological record of turtles are rareand/or damaged due to the fossilization process bias, not allowing intraspecific comparisonsor ontogenetic inferences on most fossil turtle species known (Sanchéz-Villagra & Winkler, 2006 and Ferreira et al., 2015 performed interspecific comparisons).

1.2.2. *Bauruemys* taxonomy

Bauruemys elegans (Suárez, 1969) is a Late Cretaceous freshwater side-necked turtle found at the Pirapozinho site (Suárez, 2002), in western São Paulo state. This species was originally described as *Podocnemis* in three different communications by Suárez (1969a, b, c) and identification was based on the overall similarities of the skull and shell to this living genus, a common practice at thetime. Other South American Cretaceous side-necked turtles were initially identified as *Podocnemis* as well, such as the *nomina dubia "Roxochelys" harrisi* (Pacheco,

1913) and *"Bauruemys" brasiliensis* (Staeche, 1937) and the *incertae sedis "Podocnemis" argentinensis* (Cattoi & Freiberg, 1958) (see Romano et al., 2013 for a revision on Bauru Group species and Fig. 1). Ina revision of *Bauruemys elegans*, Kischlat (1994) was the first to point out that all *Podocnemis* reported fromthe Cretaceous were doubtful and proposed a new genus, *Bauruemys*, to include *B. elegans* and, tentatively, *B. brasiliensis.* His approach was based on similarities of the plastron of both species. Kischlat (1994) and Kischlat et al. (1994) also pointed out that *B. elegans* could belong to Podocnemididae, but they did not test their hypothesis. Romano & Azevedo (2006) were the first to carry out a cladistic analysis to access the phylogenetic position of *Bauruemys*, placing it as a stem-Podocnemididae, i.e.: the sister group of all other Podocnemididae, which was confirmed by subsequent analyses withmore podocnemidid species included as terminals (França & Langer, 2006; Gaffney et al., 2011; Oliveira, 2011; Cadena, Bloch & Jaramillo, 2012).

1.2.3. Geological settings and taphonomic context of the Tartaruguito site

The Pirapozinho site, long ago known as "Tartaruguito" and formally assigned as such by Romano & Azevedo (2007) and Gaffney et al. (2011), is an Upper Cretaceous outcrop from the Presidente Prudente Formation, Bauru Basin (Geology *sensu* Fernandes & Coimbra, 2000). It is located in Pirapozinho municipality, São Paulo State, Brazil (Fig. 1). The "Tartaruguito" name, which means "turtle in rock" (*tartaruga*, from Portuguese, turtle; *ito*, from Latin, rock), is due to the great amount of turtle specimens found at that place. It is comparable to other rich fossil turtle localities, such as (1) the recently discoveredMiddle Jurassic Qigu Formation of the Turpan Basin in China (Wings et al., 2012; Rabi et al., 2013); (2) the Late Cretaceous (Maastrichtian) Hell Creek Formation ('Turtle Graveyard') in Slope County, North Dakota, USA (Lyson & Joyce, 2009); (3) the Middle-Upper Paleocene Cerrejón Formation in Colombia (Jaramillo et al.,

2007; Cadena et al., 2010; Cadena, Bloch & Jaramillo, 2012; Cadena et al., 2012); and (4) the Upper Miocene Urumaco Formation ('Capa de tortugas') in Venezuela (Aguilera, 2004; Sánchez-Villagra & Aguilera, 2006; Sánchez-Villagra & Winkler, 2006; Riff et al., 2010; de la Fuente, Sterli & Maniel, 2014). The two latter localities are near-shore marine coastal deposits with influence of freshwater rivers (Jaramillo et al., 2007; Gaffney et al., 2008), whereas the two former and the Tartaruguito site correspond to sedimentsthat had been deposited in a riverine system with seasonal droughts in which turtles gathered in retreating, ephemeral water pools and died when habitat dried up completely (Soares et al., 1980; Fulfaro and Perinotto, 1996; Fernandes & Coimbra, 2000; Henriques et al., 2002, 2005; Suárez, 2002; Murphy et al., 2003; Bertini et al., 2006; Henriques, 2006; Wings et al., 2012). The Tartaruguito is also the type-locality of the peirosauridcrocodile *Pepesuchus deiseae* Campos, Oliveira, Figueiredo, Riff, Azevedo, Carvalho & Kellner, 2011 (Campos et al., 2011).

The general lithology of the Tartaruguito site is composed of cyclic alternations of sandstones and mudstones deposited in a meandering fluvial system with crevasse splays (Fernandes & Coimbra, 2000; Henriques et al., 2005). Many articulated and complete fossils are found in these sequences, which indicate seasonal low energy floods (mudstones) followed by droughts (sandstones) in the region during the Late Cretaceous (Henriques et al., 2002, 2005; Henriques, 2006). Because only medium- to large-sized fossil specimens are found at the locality, it is assumedthat the Tartaruguito site was a foraging area for turtles (D. Henriques, pers. comm.). Thus, the fossil assemblage probably represents several episodes of floods and droughts. The flood periods might have allowed foraging areas expansion for turtles and crocodiles, while during the dry seasons turtles gathered on the remnants of water pools and some died when pools dried up completely (Henriques et al., 2002, 2005; Henriques, 2006).

That being said, we consider that all turtle specimens found at the Tartaruguito site might correspond to subadults to adult ages, and itis reasonable to assume that all *B. elegans* individuals collected in the Tartaruguito site might have belonged to a single population (agreeing with Henriques et al., 2002, 2005; Henriques, 2006) and to a single species (*B. elegans*; Romano & Azevedo, 2007). Indeed, as pointed by Romano & Azevedo (2007), this single population would consist on different generations of turtles' corpses grouped in the same locality. One might consider that size differences might be due to sexual dimorphism (R. Hirayama and S. Thomson, pers. comm.), inwhich the females would be bigger and have more posteriorly extended carapaces than the males. However, sexual dimorphism on podocnemidid turtles can be assessed only on shell shape and our data is based mostly on isolated skulls (see Material and Methods). As a consequence, although it is possible that sexual dimorphism performs a size effect in our data , we did not consider it, given the lack of evidence to assume such outcome. Moreover, Romano & Azevedo (2007) were not able to reject the single population hypothesis using shell measurements (from both plastron and carapace) in a morphometric approach neither to describe sexual dimorphism in the data, concluding that the differences were due to ontogenetic variation. Therefore, we highlight that we are assuming the population definition of Futuyma (1993), as taken on by Romano & Azevedo (2007), that a population is a conjunct of semaforonts temporally connected, i.e., a sequence of individuals from different generations, and limited in a restricted space, in this case, the Tartaruguito site. By assuming this, we explicitly follow Henning's (1966) semaphoront concept, on which a species is modifiable (i.e. not strictly typological) and represented by a sequence of generations.

1.3. Objectives

Many fossil materials are housed in foreign collections and are not easily accessible by researchers. It can narrow and even preclude their studies. In addition, given the missing data problem inherent to fossil record, the way one treatsthe missing entries in morphometric studies can affect the results and conclusions. Regarding the use of caliper or ImageJ in taking measurements, here we (1) tested both approaches by taking linear measurements for morphometric studies based on photographs (e.g. Bailey, 2004) and also (2) evaluated how different approaches designed to deal with missing data can impact results of exploratory statistical procedures and data interpretation by comparing two different substitution algorithms of missing entries. These procedures are exemplified using a real paleontological data set and with paleobiological inferences.Considering the case-study, we (3) explored the variation in skulls among individuals of *Bauruemys elgans* from different ages and generations. and (4) described the differences in skull morphology along the ontogeny of the speciesand discuss the probable consequences of such variation to the diet preferences changes along the growth.

2. Material and Methods

2.1. Sample and characters

Twenty-one skulls of *Bauruemys elegans* were examined in this study: AMNH-7888, LPRP0200, LPRP0369, LPRP0370, MCT 1492-R (holotype), MCT 1753-R (paratype), MCZ 4123, MN 4322-V, MN 4324-V, MN 6750-V, MN 6783-V, MN 6786-V, MN 6787-V, MN 6808-V, MN 7017-V, MN 7071-V, MZSP-PV29, MZSP-PV30, MZSP-PV32, MZSP-PV34, and MZSP-PV35. We established 39 landmarks (Fig. 2) that decompose the overall shape of the skull in order to take measurements between two landmarks. Moreover, since most of the specimens have deformation and breakage, we could not perform a geometric morphometric analysis using

the landmarks because the taphonomical bias would incorporate error to the analysis of form and shape. Thus, we used the landmarks to set up 29 traditional morphometric characters that correspond to a linear measurement between two landmarks (all characters are described in table 1). Also, the use of landmarks to set up the measurements is useful to maintain the same anatomic references for all characters in each specimen, since the landmarks enable a better description of morphological variation and establishment of quantitative characters, as exemplified by Romano & Azevedo (2007). All measurements were taken on the same side of the skull (right side) unless the characters could not be measured due to deformation or breakage. We are aware that deeper structures (z-axis) can influence the straight line between two landmarks in 2D images and used ImageJ version 1.47 (Rasband, 1997) to take the measurements after comparing its accuracy with the caliper (Mariani & Romano, 2014). This procedure was necessary because weobtained photos of skulls in dorsal, ventral and lateral views housed in foreign collections and did not perform measurements by caliper. The error test between measurements taken using caliper and ImageJ are described below. We followed the bone nomenclature of Parsons & Williams (1961) and extended by Gaffney (1972, 1979) (see all abbreviations after Conclusion topic).

2.2. Statistical analyses

2.2.1. Preliminary analysis: Caliper vs. ImageJ

Before carrying out others statistical analyses, we compared the same characters data set (Data S1) of the same sample by using two different approaches (= treatments): measurements taken using caliper and measurements taken using photographs via ImageJ. This comparison was necessary in order to evaluate whether or not the two measurements methods are significantly

different. Then, we performed an One-way Analysis of Variance (ANOVA) comparing the 29 measurements in 12 specimens (LPRP0200, LPRP0369, LPRP0370, MN4322-V MN4324-V, MN6750-V, MN6783-V, MN6786-V, MN6787-V, MN6808-V, MN7017-V, and MN7071-V). Two groups of variables were established: measurements taken directly from specimens using caliper (preliminary data set 1) and the same characters taken from photographs of the same specimens using ImageJ (preliminary data set 2). All characters taken using photographs/ImageJ that did not show significant differences to their correspondents taken by caliper were used on the subsequent statistical analyses of form and shape differences among the sample of *Bauruemys elegans*. By doing that, the sample was increased without including error and incomparable characters (i.e.: by using different measurement techniques).

We found most of the measurements do not differ statistically ($p>0.05$) between the two treatments (caliper and ImageJ; table 1). However, one measurement, length of maxilla (LMX), had statistical difference ($p=0.017$) between the treatments, because the maxilla is a curved structure and thus the landmaks are in different positions (LM 24 is deeper and farther from the camera in relation to LM11) in relation to the plane the picture was taken. Given that no statistical differences were found in almost all characters, the ImageJ could be an economic and time-saving tool for morphometric analyses from photographs (2D), and could be applied by scientists at distant institutions.

Despite this, the study *in situ* of the material is preferable, although pictures are an economic alternative in cases one is not able to handle the material. We must aware that one have to choose one of the two treatments to construct a morphometric matrix, otherwise it will be composed of values obtained by two diffent methods.

196 **2.2.2. Univariate, multivariate and allometric analyses**

197 Three analyses using the complete sample were carried out: (1) a descriptive statistics (mean,
198 standard deviation, median, variance, maximum and minimum values) of all characters (Data
199 S2), (2) an allometric analysis of length and width characters correlating them to total length and
200 width measurements (Data S3), and (3) a multivariate non-parametric exploratory statistics via
201 Principal Component Analysis (PCA). The latter was divided into two different PCAs: (3.1)
202 using 27 characters from the raw data matrix (total length and width characters were excluded in
203 this analysis; Data S4), and (3.2) using 27 charactes that correspond to the proportions of each
204 character from the raw data (i.e. original measurements) represented by its length orwidth
205 characters divided by each individual total length orwidth (e.g. the length of MCZ4312
206 postorbital divided by the total length of the skull of this specimen; see complete data in Data
207 S5). All statistical analyses were performed using the software PAST version 3.05 (Hammer et
208 al., 2001).

209 In the allometric analysis (analysis 2, Data S3), all characters were previously log-transformed
210 and a linear regression was carried out separately for length and width characters, using the least
211 square fitting approach for residuals. We established the allometries by considering the
212 regression's slope, i.e. the coefficient a, as following: positive allometry ($a>1$), negative
213 allometry ($1>a>0$), truly negative allometry ($a<0$), and isometry ($a=1$).

214 In the first PCA approach (3.1) we excluded total length and width characters because of its high
215 influence on the PCA result, since higher values compose the majority of the summarized
216 variance in PC's (Mingoti, 2013), and because of the redundance between these measurements
217 and the others. We also assessed differences by applying two different substitution algorithms for

missing data in PAST, using the default "mean value imputation" option (i.e. missing data are replaced by the column average), and the alternative "iterative imputation" option, which computes a regression upon an initial PCA until it converges to missing data estimations, replacing missing data by such estimations (Ilin & Raiko, 2010). The latter is recommended and, after comparing both results, we selected it (see supplemental material 3 to visualize PCA results computed using PAST's default option approach). The second PCA (3.2) was conducted to remove the effect of size (=growth) and perform an exploratory analysis of the shape alone. Six specimens were removed from this analysis because they were broken and the total length or width measures were not measurable.

The univariate analysis was made in order to quantify and describe the variation of the characters set in *Bauruemys elegans* skull, using the assumption of the sample be representative of a single population. The linear regression analyses allowed us to make inferences about osteological shape change related to size change, i.e., related to growth, by assuming that bigger specimens are older than smaller ones. This approach is, therefore, a study of allometry (Huxley & Teissier, 1936; Huxley, 1950; Gould, 1966; Gould, 1979; Somers, 1989; Futuyma, 1993) and the assumption of correlation between size and aging is based on continuous growth to be common on extant turtles (Klinger & Musick, 1995; Shine & Iverson, 1995; Congdon et al., 2003). Since the use of a parametric statistic was infeasible due to the nature of the sample (i.e.: a small matrix that do not show homoscedasticity and normality in data set), the PCAs were used to search for a structure of the data that matches to the pattern found by Romano & Azevedo (2007) using postcranial characters (i.e. all individuals plotted inside the 95% confidence ellipse). If the pattern observed is similar to previous morphometric and taphonomic inferences, then the variation is not enough to assume that the sample represents different populations of *Bauruemys*

241 *elegans* or a different species (see section 4.1.2). In other words, since a parametric test is not
242 feasible with statistical confidence, the lack of structure in the PC plots were herein interpreted
243 as a fail to the attempt of falsifying the single population hypothesis.

244 **3. Results**

245 **3.1. Descriptive Analysis**The results of the descriptive statistics are summarized in table 2. As
246 expected, values of total length and width (TLS and WLS) were the most variable in comparison
247 with others, because the variation scale in these characters is greater than in others. Characters of
248 the bones forming the upper temporal fossa (i.e. PA, QJ, SQ, QU and OP) had great variation,
249 with the parietal being the most variable in length (SD=6.45) and the least variable in width
250 (SD=2.94), whereas quadratojugal obtained the smallest variation in length (SD=2.38) and the
251 greatest in width (SD=4.03). Among the characters of the bones forming the lower temporal
252 fossa (i.e. JU, MX, PO, PT and PAL), the variation in length was in general greater than in
253 width. Postorbital and maxilla had almost the same variation in length (SD=4.12 and SD=4.11,
254 respectively); WPO had the smallest variation within the group of bones forming the lower
255 temporal fossa (SD=1.83); and the stretch of the maxilla had the greatest variation (SD=7.63) of
256 all characters measured. Characters of the other bones had smaller values than the
257 aforementioned bones, with the exception of WPO which was smaller than LFR (SD=2.08),
258 LVO (SD=1.95), LBO (SD=2.12),WFR (SD=1.88) and WBS (SD=2.19).

259 **3.2. Allometric Analysis**

260 Among all comprised measurements, three were truly negatively allometric (LPF, WJU and
261 WQJ); five were positively allometric (LPAL, LPT, LPO, WPF and WPO); and the others were
262 negatively allometric. It is also worth to note that two were not isometric [WPF (a=1,0074;

263 p=0.0009) and WOP (a=0.98159; p=0.007)], although presented angular coefficient very close to
264 1. All regressions are shown in figures 3, 4 and 5.

265 **3.3. Principal Component Analysis (PCA)**

266 **3.3.1. Raw data**

267 **3.3.1.1. Replacing missing data with mean values**

268 By using the "mean value imputation" approach, a total of 70.32% of the variance was
269 comprised by the first three principal components (PC1=42.15%; PC2=16.82%; PC3=11.35%),
270 so that the others were less significant for the analysis by following the broken stick model, and
271 are not presented. We interpreted that PC1 variation is due to size change because an approach
272 using all characters has shown a similar plot (see Fig. 6A).. PC2 and PC3 seems to represent
273 shape differences between individuals. In all PC individual projections (Fig. 6A and 6B) most of
274 specimens were included inside the 95% confidence ellipse. Two exceptions are MCZ4123 and
275 MN7071-V, which have not been included in the ellipse when PC1 vs. PC2 were considered
276 (Fig. 6A); also the former was outside the ellipse in PC2 vs. PC3 scatter plot (Fig. 6B),
277 indicating shape differences of these specimens. However, both specimens have suffered
278 different degrees of crushing due to taphonomic bias and that is likely the reason for this result.

279 In PC1' loadings (L; Table 3), only two characters were negatively related (LPF and WJU);
280 SMX, LPA and LPO loadings were the highest related (L=0.69; L=0.27; L=0.36, respectively);
281 and the rest of characters obtained intermediate values [e.g. LPT (L=0.17), LMX (L=0.18), WOP
282 (L=0.21)]. PC2 has shown a high relation with character LPA (L=0.77), showing possible
283 changes in shape in this region, and a negative loading for SMX (L= -0.38), whereas the others
284 had no significant scores. The last considered principal component (=PC3), showed high

correlations with bones in both lateral and posterior emarginations of the skull [LMX (L=0.68), WMX (L=0.25), LJU (L=0.30), WQJ (L=0.29) and LQU (L=0.32)] and, as the results in PC2, allows inferences in shape changes of these regions.

3.3.1.2. Replacing missing data with regression estimation

The alternative missing data approach (i.e. "iterative imputation"; Fig. 6C) generated two principal components which comprised 88.96% of the total variance (PC1=53.01%; PC2=35.95%). In contrast with the previous approach, PC1 was interpreted as representing shape and PC2 size. In addition, all specimens were included inside the 95% ellipse in PC1vs.PC2 scatter plot. The specimen MN7017-V, interestingly, was excluded from the ellipse when considering PC2 vs. PC3, but the percentage of variance represented by PC3 is too low (PC3=3.28%) to assume any difference from the others individuals. We agree with Ilin & Raiko (2010) and prefer to choose the iterative imputation approach for dealing with missing entries (see discussion on session 4.2. "The single population hypothesis"). Then, discussions concerning the form variation in our data are related to PCA analysis using iterative imputation.

In PC1 loadings (Table 3), LPA, WPA and LSQ were the highest positively related characters (L=0.89; L=0.22; L=0.16, respectively), whereas LMX, LJU, LQJ, WQJ and LQU were the highest negatively related characters (L= -0.18; L= -0.14; L= -0.16; L= -0.11; L= -0.11; L= -0.13, respectively). Only two characters were negative for PC2 (LPF and WJU), whereas the rest of the coefficients were positive. Among them, SMX was the highest (L=0.59); WPAL, WBS, LBO, LJU, LQU, LPO and WOP obtained intermediate scores (L=0.23; L=0.19; L=0.20; L=0.19; L=0.21; L=0.29; L=0.30, respectively); the others were less related [e.g. LPA (L=0.04),

306 LPT (L=0.13) and WPO (L=0.10)]. In general, the values indicate that in *B. elegans* most
307 changes occur in bones of both lateral and temporal emargination.

308 **3.3.2. Shape characters (proportions)**

309 **3.3.2.1. Replacing missing data with mean values**

310 When applying "mean value imputation", 53.99% of the variance were comprised by the first
311 two principal components (PC1=35.29%; PC2=18.70%), both corresponding to shape, as all
312 units of measurements were removed through the division of characters before carrying out the
313 analysis. All specimens were comprised into the 95% confidence ellipse (Fig. 7A).

314 The first PC was positively related to the loadings values of LPA/TLS (L=0.28), LMX/TLS
315 (L=0.38), LQU/TLS (L=0.27), WPA/TWS (L=0.23), SMX/TWS (L=0.38), WMX/WTS
316 (L=0.35), WQJ/TWS (L=0.48); the most negative values were LPO/TLS (L= -0.16) and
317 WOP/TWS (L= -0.13). The second PC was positively related to LPA/TLS (L=0.66), WPA/TWS
318 (L=0.32)WOP/TWS (L=0.27), and negatively to LMX/TLS (L= -0.50) (see Table 4 for all
319 loading values). It is interesting to note that most of highly-related proportions were in reference
320 to bones associated either with feeding *apparatus* (squamosal, parietal, quadratojugal and jugal)
321 or catching food and trituration surface (maxilla).

322 **3.3.2.2. Replacing missing data with regression estimation**

323 The "iterative imputation" substitution model of missing data explained 77.35% of the variance
324 comprised by two principal components (PC1=45.49%; PC2=31.86), both representing shape.
325 All specimens were included in the confidence ellipse (Fig. 7B), thus shape differences do not
326 indicate possible different populations or species.

PC1 was highly related to LMX/TLS (L=0.48), LJU/TLS (L=0.16), LQJ/TLS (L=0.21), LQU/TLS (L=0.28), LSQ/TLS (L=0.20), SMX/TWS (L=0.33), WMX/TWS (L=0.30), WJU/TWS (L=0.26) and WQJ/TWS (L=0.41), which represent the highest values, as well as bones constituting both lateral and posterior emargination. Conversely, PC2 was mostly represented by LPA/TLS (L=0.67), LSQ/TLS (L=0.34) and WPA/TWS (L=0.33) (see Table 4). These loadings represent shape changes in regions of the skull that are associated with muscles' attachments as well as trituration surfaces (see below).

4. Discussion

4.1. The single population hypothesis

In this section, we discuss the single population hypothesis considering two fronts, one underlied on the taphonomy of the Tartaruguito locality, and another on the possibility of the skull variation represent the species *Roxochelys wanderleyi*, a shell-only species also found at the site.

4.1.1. The depositional context at the "Tartaruguito" site

The depositional environment at the Pirapozinho site is well-known from previous studies, which point out to seasonal floods in which turtles might have gathered in water bodies for foraging, followed by droughts that caused their death (Soares et al., 1980; Fulfaro and Perinotto, 1996; Fernandes & Coimbra, 2000; Henriques et al., 2002, 2005; Suárez, 2002; Bertini et al., 2006; Henriques, 2006). This is, consequently, a case of several seasonal non-selective death events, with individuals representing semaphoronts connected temporally (between generations), thus comprising a single population (agreeing with Futuyma, 1993 population definition and used by Romano & Azevedo, 2007). We failed to disprove the null hypothesis that all individuals belong

348 to a same population of *Bauruemys elegans*, agreeing with Romano & Azevedo (2007)
349 conclusion using post-cranium data.

350 *4.1.2. Taxonomic considerations on the sample*

351 Many skulls sampled showtaphonomic effects, such as cracks and crushings (Fig. 8). For
352 instance, MN7071-V is notably the largestspecimen of the sample and is represented in the
353 uppermost positive side of the size-related PC2 axis (Fig. 6C). Although it is indeed a big
354 specimen, it was clearly a taphonomic effect (crushing) that caused it to be largerthan it real was
355 (Fig. 8A). On the other hand, Bertini et al. (2006) indicated that turtle bodies have suffered little
356 transportation or crushing in Tartaruguito site. We agree with this taphonomical interpretation of
357 the site, as most specimens do not show huge breaks (Fig. 8B and 8C) that could cause
358 misinterpretation of the morphometric results (the case of MN7071-V is an exception in our
359 sample in this respect).

360 Another aspect is the presence of polymorphism in *B. elegans*. Romano (2008) presented an
361 unusual carapace for the specimen MN7017-V, as having a seventh neural bone, differing from
362 the diagnostic number of six neurals for this species, and with the diagnostic four-squared second
363 neural bone not contacting first costals (Suarez, 1969; Kischlat, 1994; Gaffney et al., 2011). The
364 morphometric analysis performed by Romano (2008) did not reveal significant statistical
365 differences between MN 7017-V and other *B. elegans* specimens. We have included the
366 MN7017-V skull in our analysis, and there was no variation to state anything apart from
367 Romano's (2008) conclusion that it is probably a polymorphic *B. elegans* specimen (Fig. 6C).
368 Still, we reevaluated this skull and found the diagnosic characters for *B. elegans*. Therefore, all
369 skulls included in our study belong to the same species (i.e. *B. elegans*).

Among the five valid fossil turtle species found throughout the Bauru Basin, only two have been collected at the Pirapozinho site so far (Romano et al., 2013). The first is *B. elegans*, which is recognized by both skull and shell materials; the second is *Roxochelys wanderleyi* Price, 1953, based only on shell material (de Broin, 1991; Oliveira & Romano, 2007; Romano & Azevedo, 2007; Gaffney et al., 2011; Romano et al., 2013). So far, none *R. wanderleyi* with skull-shell associated body parts were collected, and thus we cannot claim that the skulls found at Tartaruguito site belong to this species until a skull-shell *R. wanderleyi* specimen be found.

4.2. Ontogenetic changes in *B. elegans* skull

Once we have assessed that all specimens belong to the same species and are likely from the same population, we are able to discuss the skull variation in the sample assuming as due to inter-populational variety. For the sake of organization, we divided the discussion into two parts, based on the anatomical regions of the turtle skull: upper temporal fossa and lower temporal fossa, following Schumacher (1973), Gaffney (1979) and Gaffney et al. (2006). We have chosen this organization because the bones we found most associated with the principal components in the two PCA analyses constitutethese two regions and are generally involved in aspects of the feeding mechanisms of turtles, either as muscles attachments or forming triturating surfaces.

4.2.1. Bones of the upper temporal fossa and skull roofing

The temporal emargination of podocnemidid turtles is formed by the dorsal, horizontal plate of the parietal, the quadratojugal and the squamosal, with no contribution of the postorbital (Gaffney, 1979; Gaffney et al., 2011). This region (and bones) is associated withthe origin of the adductor muscle fibers (m. adductor complex; Fig. 9A and 9B) (Schumacher, 1973; Werneburg, 2011; Werneburg, 2012; Jones et al., 2012; Werneburg, 2013), which run through *cartilago*

392 *transiliens* of the *processus trochlearis pterygoidei* of the pterygoid and insert at the coronoid
393 process of the lower jaw (Schumacher, 1973; Gaffney, 1975; Gaffney, 1979; Lemell et al., 2000;
394 Werneburg, 2011). These muscles promote the closure of the mouth, thus it is reasonable to
395 associate the attachment surface to bite force and the latter to the prey hardness. Yet, on the
396 ventral flange of the squamosal originates the m. depressor mandibulae (Schumacher, 1973;
397 Gaffney et al., 2006; Werneburg, 2011; Fig. 9B), which causes the abduction (=opening) of the
398 mandible.

399 The variation in this area of the skull in turtles was a matter of some studies (e.g. Dalrymple,
400 1977; Claude et al., 2004; Pfaller et al., 2011), which indicated allometric ontogenetic growth
401 patterns of the bones in these regions. Theseauthors were able to identify a high correlation with
402 the increasing of muscle mass and shift in feeding features (Dalrymple, 1977; Pfaller et al., 2010;
403 Pfaller et al., 2011). Moreover, there are changes in skull shape associated to the aquatic
404 environment and foraging strategies, as suggested for emydid and testudinoid turtles by Claude
405 et al. (2004). Although these studies focused on hide-necked turtles, the same morphoecological
406 patterns can be applied to side-necked turtles, since there are habitat occupation similarities
407 between side-necked and hide-necked turtles with implications to the skull morphology due to
408 morphofunctional constraints (Schumacher, 1973; Lemell et al., 2000), besides the adaptive
409 selection regarding fresh water feeding strategies (see Lauder & Prendergast, 1992, Aerts et al.,
410 2001 and Van Damme & Aerts, 2001 for feeding strategies in freshwater turtles).

411 The high variance and positive allometric growth of the parietal (LPA: a=0.38; WPA: a=0.32),
412 quadratojugal (LQJ: a=0.16; WQJ: a= -0.06) and squamosal (LSQ: a=0.30) lead to an increase in
413 temporal emargination and, consequently, a greater area for attachment of the m. adductor
414 mandibulae externus. The consequence of this would be the generation of large forces and high

velocities during the fast closing phase of an aquatic feeder, as seen in *Pelusios castaneus* (Lemell et al., 2000), and even a more powerful bite for crushing harder prey, as seen in *Sternotherus minor* (Pfaller et al., 2011). In addition, the lengthhen of the squamosal would allow a greater insertion area of the m. depressor mandibulae and muscles of the hyobranchial apparatus (e.g. m. *constrictor colli*) (Schumacher, 1973; Gaffney, 1979; Claude et al., 2004; Gaffney et al., 2011; Werneburg, 2011). The m. depressor mandibulae is useful for an increased gape opening speed and the hyobranchial apparatus musculature is involved in backwards water flow generation by the lowering of the hyoid apparatus, two characteristics well reported for other pleurodire turtles (e.g.Van Damme & Aerts, 1997; Aerts et al., 2001; Lemell et al., 2000; Lemell et al., 2002). Moreover, Claude et al. (2004) demonstrated that aquatic turtles with suction feeding mode possess longer skulls than terrestrial turtles, the squamosal being most proeminent bone involved in this elongation and functionally related to the style of prey capture (= suction) as a support for mandible and hyoid muscles.

Also, Gaffney et al. (2011), in a comparison with other podocnemidid turtles, indicated *B. elegans* as having a "skull relatively wide and flat" (p. 12), which could be observed by the increasing of some bones, specially the postorbital (Figs. 3G and 4H), parietal (Fig. 3A and 3J), quadratojugal (Figs.3I and 4F) and jugal (Figs. 3C and 5B). Comparing the postorbital allometry (better discussed below) with those of the bones in contact with it in the skull roof (frontal, parietal, jugal and quadratojugal; Gaffney et al., 2011), we observe an influence of the positive growth of the former into the others, leading to flattening and widening of the skull.

In a study assessing the bite performance in turtles, Herrel et al. (2002) suggested that a higher skull is efficient in promoting stronger bite forces, specially in species which feed on hard prey, but they also pointed out that additions in bite forces may be achieved by "getting longer and

larger" skull with no increasing in skull height. Thus, in addition to provide gains in muscle attachment area, by the growing of parietal, quadratojugal and squamosal, leading to a longer skull, a stronger bite and possibly a change in diet along the ontogeny. Also, the allometric growths of most of skull bones, particularly the positive allometry of the postorbital, indicate a more roofed skull in *B. elegans* adults. Given the allometric patterns aforementioned, *B. elegans* may have had a wide and flat but a long skull, which would have compensated the loss of muscle volume and attachment area caused by widening and flattening the skull (Herrel et al., 2002). Correlations between a more emarginated skull and increases in the volume of the adductor muscles were also explored in a cranial evolutionary framework of stem-turtles by Sterli and de la Fuente (2010).

At last, Gaffney et al. (2006, 2011) scored a character based upon the contact between quadratojugal and parietal bones (char. 13 of Gaffney et al., 2006; char. 5 of Gaffney et al., 2011). They also state that this contact is present in *Hamadachelys* + Podocnemididae clade, with a large quadratojugal (state 1), in contrast to most of other Pelomedusoides (state 0: contact absent in Pelomedusidae, Araripemydidae and many bothremydids (e.g. Kurmademydini, Cearachelyini and Bothremydini); state 2: contact present with small quadratojugal in some Taphrosphyini, Bothremydidae). Indeed *B. elegans* possess a large quadratojugal, which means that the reduction of the postorbital evolved after *Bauruemys* node of divergence. However, we found a greater increasing (positive allometry) of the two measurements of the postorbital and this might have influenced the growth of parietal and quadratojugal, as well as the jugal (see below), so that the state 1 seen in *B. elegans* is possibly a consequence of allometric changes. This is easily seen if the truly negative allometry of the width of the quadratojugal (WQJ: a=-0.06) and the slight increasing in the length of this bone (LQJ: a=0.16) are compared with the

postorbital measurements. It also could have influenced the growth of the parietal, but to a lesser extent, as seen in the allometries of this bone (LPA: a=0.38; WPA: a=0.32).

When comparing the stem-Podocnemidinura species (i.e. *Brasilemys*, *Hamadachelys*) and stem-Podocnemididae (e.g. *Bauruemys*, *Peiropemys*, *Pricemys* and *Lapparentemys*), with the Podocnemidodda (i.e. Podocnemidand + Erymnochelydand) (Gaffney et al., 2011; Fig. 8), it is clear that an increasing in the parietal-quadratojugal contact has occurred along the podocnemidid lineage, and consequently led to a more roofed skull and less emarginated skull. We suggest that in *B. elegans* the small contact is due to the positive growth of the postorbital resulting in a more emarginated skull than other podocnemidids, as described by Gaffney et al. (2011). Yet, within Podocnemidand this bone suffered the opposite effect (i.e. small growth), showing variations in size and even being absent in some species (e.g. *Podocnemis sextuberculata*; Ruckes, 1937; Gaffney, 1979; Gaffney et al., 2011), though the emargination is still great. On the other hand, in Erymnochelydand the postorbitals are large but the quadratojugal and parietal are large as well, leading to a greater contact between these bones and a well-roofed but less emarginated skull, being a reversion in *Bairdemys venezuelensis* and *B. sanchezi* within Erymnochelydand (Gaffney et al., 2011). Therefore, the increase or decrease in the temporal emargination within Podocnemididae could be due to variation of allometric patterns in bones that form the skull roof, particularly the postorbital, quadratojugal and parietal, among different lineages.

4.2.2. Bones of the lower temporal fossa

The lower adductor chamber in Pelomedusoides is formed externally and laterally by the jugal and quadratojugal, with the addition of the maxilla in some cases (e.g.: *Podocnemis* spp. and

Bairdemys sanchezi). The well developed cheek emargination, found in most but not all podocnemidid turtles (the exceptions are many species of Erymnochelydand, but not *Bairdemys* spp., *Cordichelys antiqua* and *Latentemys plowdeni*), is also part of the adductor chamber (Gaffney, 1979; Gaffney et al., 2006; Gaffney et al., 2011). Internally and medially, the postorbital, the jugal and the pterygoid compose the *septum orbitotemporale*, partially separating the *fossa orbitalis* from the *fossa temporalis*; along with the palatine, they aid to support the *processus trochlearis pterygoidei* of the pterygoid (Gaffney, 1975; Gaffney 1979; Gaffney et al., 2006). There is a passage medially to the process of the pterygoid and the *septum orbitotemporale*, running from the *fossa orbitalis* to the *fossa temporalis*, the *sulcus palatinopterygoid*

eus. The palatine and pterygoid form the floor of its passage, whereas the parietal, postorbital and frontal limit its upper portion. In this region, the m. adductor mandibulae fibers run through the *processus trochlaris pterygoidei*, and the m. adductor mandibulae internus (i.e. m. pterygoideus and pars pseudotemporalis; Fig. 9B) mostly originates throughout the pterygoid and parietal bones (Schumacher, 1973; Lemell et al., 2000; Lemell et al., 2002; Werneburg, 2011). The m. adductor mandibulae internus fibers are involved in the jaw-closure system by generating counter forces (protraction) to the m. adductor mandibulae externus (retraction) (Schumacher, 1973; Lemell et al., 2000; Lemell et al., 2002; Fig. 9C and 9D).

Variation of the upper temporal fossa has been studied in different turtles, such as various trionychids (Dalrymple, 1977) and *Chelydra serpentina* (Herrel et al., 2002). However, few studies report on the variation of the lower adductor chamber, although both the upper temporal fossa as well as the lower temporal fossa are anatomically and functionally coupled (Schumacher, 1973). Dalrymple (1977) identified a positive allometry in the width of the

506 "temporal passageway" in trionychids. This area is related to the cryptodire pulley system (i.e. a
507 *processus trochlearis* formed by the quadrate and opisthotic) and is analogous to the pleurodire
508 pterygoid process, and thus can be comparable functionally (Gaffney, 1979). Herrel et al. (2002)
509 concluded that the increase of the bite force in turtles is due to either the increased height of the
510 skull, leading to a more open angle of the *processus trochlearis* in relation to skull longitudinal
511 axis, or to enlargement (in width and length) of the skull, because it allows more area for muscle
512 attachment and volume. We observed the same pattern of growth change in *B. elegans*, as
513 evidenced by the positive allometry of the parietal, postorbital, palatine and pterygoid bones.
514 Other features were observed by Dalrymple (1977) in trionychids (e.g. height and width of the
515 supraoccipital crest, lengthening of the squamosal crest and a development of a horizontal crest
516 in the parietal) and were correlated to changes in skull shape with a shift in feeding habits, from
517 softer to harder preys as individuals age. Again, this seems to be the case in *B. elegans*, as
518 evidenced by the positive allometry of the squamosal and parietal bones.

519 The bones that mainly compose the skull rostrolaterally and the lateral emargination revealed a
520 correlated allometric shape shift. Even so, jugal and maxilla showed small allometric variation
521 (Figs. 4B, 4C, 6A, and 6B). The reduction of the jugal (WJU: a= -0.23) and quadratojugal (WQJ:
522 a= -0.06) along with the small growth of the maxilla (WMX: a=0.19) demonstrate a decrease in
523 height at the anterior portion of the skull. Because of the contact between jugal and quadratojugal
524 with the postorbital (and its increase; see previous topic), we suggest that the latter would
525 possibly has affected the growth of the former bones. Moreover, the strong development of the
526 postorbital would ultimately affect the width of the maxilla, which in turn would also affect the
527 jugal. In contrast, the lengthen of this bone would be less affected (LMX: a=0.39). In addition,
528 there is a considerable increment in the stretch of maxilla (SMX: a=0.70) (Fig. 3H) leading to a

broader rostrum. Yet, this could allow a greater area for crushing (Kischlat, 1994) during ontogenetic growth. All these allometric changes indicate that *B. elegans* owns a more flattened and wider skull (Gaffney et al., 2011), which could have allowed greater bite forces generation (Herrel et al., 2002).

There are other morphological implications in which the lower adductor chamber bones are involved and that are worth discussing. As previously pointed out, three bones compose the *septum orbitotemporale*: pterygoid, jugal and postorbital (Gaffney, 1979; Gaffney et al., 2006). Together with the palatine, these three bones provide support for the *processus trochlearis pterygoidei*, whereupon runs the tendon that connect the m. adductor externus complex into the lower jaw (Schumacher, 1973; Gaffney, 1975; Gaffney 1979; Lemell et al., 2000; Gaffney et al., 2006; Werneburg, 2011). Nearby the process, many muscle fibers originate or cross towards their insertions points (Schumacher, 1973; Werneburg, 2011). The temporal emargination at the upper adductor chamber becomes more emarginted during growth. As a consequence, the attachment area for m. adductor mandibulae externus increase during aging, potentially generating stronger bite forces. The consequence of this temporal emargination indentation is that the trochlear process would must become more robust to support higher forces. We interpret that the positive allometries of pterygoid (LPT a=1.37), postorbital (LPO a=1.25 and WPO a=1.36), and palatine (LPAL a=1.11) could be a response to this robustness of the trochlerar process during growth. In other words, they would act together by giving more resistance to the area in which the high forces created by the m. adductor mandibulae externus are applied. Gaffney (1979) suggested this robustness occurs because muscle volume increase and, consequently, higher bite forces, so these three bones would reinforce the *septum orbitotemporale* in order to support and do not break when muscles are contracted. In addition to

552 such reinforcement, the growth of palatine could be associated with a larger area for crushing
553 preys such as mollusks and crustaceans, as pointed out by Kischlat (1994).

554 The m. adductor mandibulae internus and m. adductor mandibulae posterior (Fig. 9B), which
555 originate at the quadrate, prootic, pterygoid, palatine, postorbital and the descending process of
556 the parietal (Schumacher, 1973; Werneburg, 2011), are important during the jaw-closure phase.
557 The importance of these muscles has been debated for early tetrapods with flat skull and aquatic
558 lifestyle (e.g. Temnospondyli and Lepospondyli; Frazzetta, 1968), in which the internal muscle
559 might have assumed the main function of closing the jaw (Werneburg, 2012). This also occurs in
560 turtles with flat skulls and with poorly developed crista supraoccipitalis (e.g. Chelidae;
561 Werneburg, 2011; Werneburg, 2012). However, *B. elegans* does not have a skull as flat as
562 chelids, but has a long supraoccipital bone as well as a greater temporal emargination (Gaffney et
563 al., 2011), indicating more area and volume avaiable to m. adductor mandibulae externus
564 (Dalrymple, 1977; Sterli & de la Fuente, 2010). The mechanical effects of adductor muscles
565 upon the lower jaw during food capture has been demostrated in some turtles (Schumacher,
566 1973; Lemell et al., 2000; Lemell et al., 2002; Pfaller et al., 2011). These studies agree that
567 besides acting to close the mouth, the m. adductor mandibulae internus executes counter
568 protraction forces to the m. adductor mandibulae externus retraction forces, while m. adductors
569 mandibulae posterior produce medial forces (Fig. 10C and 10D). The contraction of all these
570 muscles together avoid displacements of the mandible and reduce stresses at the articulation
571 (Schumacher, 1973; Lemell et al., 2000; Lemell et al., 2002). The positive allometries of the
572 bones of the lower adductor chamber of *B. elegans*, therefore, may reflect greater resistance for a
573 more robust musculature of m. adductor mandibulae internus and m. adductor mandibulae
574 posterior in response to higher forces created by external adductors. Besides, these muscles also

play the main role in feeding, as proposed for aquatic feeders (Frazzetta, 1968; Werneburg, 2012), in addition to a larger area between the two tips of the maxilla (i.e. SMX a=0.70) and a flattened skull.

4.3. Feeding changes over ontogeny in *B. elegans*

Changes in skull shape may be due to habitat differences in which terrestrial turtles (e.g. testudinids) possess higher and shorter skulls while aquatic turtles (e.g. emydids) have flatter and longer skulls (Claude et al., 2004). The changes in skull shape of turtles along ontogeny have been assessed in living species (Dalrymple, 1977; Pfaller et al., 2011). Generally, it is supported that a diet shift occurs from small soft prey to bigger harder ones, in association with higher, larger and more robust skulls. These, in turn, are more suitable for crushing clams and/or to capture fishes by having a greater gape. The overall aquatic morphology comprises adaptations to suction feeding, which was also discussed by Herrel et al. (2002), and could be the case of *B. elegans*. Firstly because taphonomic studies at Pirapozinho site suggested a riverine ephemerous system (Soares et al., 1980; Fulfaro and Perinotto, 1996; Fernandes & Coimbra, 2000; Henriques et al., 2002, 2005; Suárez, 2002; Bertini et al., 2006; Henriques, 2006) and fossils with little transportion (Bertini et al., 2006), thus *B. elegans* must have been a semi-aquatic turtle, similar to the extant freshwater turtles. Secondly, the general pattern observed revealed form and shape changes in both temporal and lateral emargination (upper and lower adductor chamber, respectively): as a whole, *B. elegans* skull seems to become more emarginated, flattened and longer as it grows, according to the skull shape for aquatic turtles found by Claude et al. (2004), and indicating greater area and volume for muscles attachment. In addition, the deeper temporal emargination of *B. elegans* indicates a greater increase in muscle volume (Kischlat, 1994), thus

leading to a stronger bite force (Sterli & de la Fuente, 2010). This leads us to interpret such changes as related to a shift in diet as individuals grow instead of a shift in habitat.

Malvasio et al. (2003) described diet changes in *Podocnemis expansa*, *P. unifilis* and *P. sexturberculata* due to aging, concluding that the latter is a carnivore species, whereas the two former are omnivorous. Whereas *P. expansa* changes its diet becoming more herbivorous, *P. unifilis* remains more balanced with similar ingestion of vegetables and meat (Malvasio et al., 2003). Kischlat (1994) suggested that *B. elegans* might have fed of hard preys and, given the several mollusk and crustacean species described for the Pirapozinho site (Dias-Brito et al., 2001), it might have composed the diet of *B. elegans*. In this context, we agree with Kischlat (1994) and suggest that smaller juveniles individuals might have fed on less hard and small food itens (e.g. snails and small fishes) whereas bigger old specimens fed on harder and larger preys, such as crustaceans and bigger mollusks.

Although there is a possibility that size differences could be due to sexual dimorphism (R. Hirayama and S. Thomson, pers. comm.) as aforementioned (see Introduction, section 1.2.3), we were not able to assume such an assumption. Furthermore, if there is size-related dimorphism, it would imply on potential diet differentiation between adults male and female of *B. elegans*. Since we were not able to determine size-related sexual dimorphism, such hypothesis is merely speculative.

5. Conclusions

As Romano & Azevedo (2007) (for shell material), our data did not show enough morphometrical variation to suggest population differences among our sample. So, we did not have evidence to disprove that the "Tartaruguito" site is composed of a single population of *B.*

619 *elegans*. However, it is feasible to assume that different generations of individuals were crowded
620 in this locality by the accumulation of corpses due to several drying events as previously
621 suggested by Henriques et al. (2005) and Henriques (2006). Since none *B. elegans* hatchling
622 were found in the "Tartaruguito" site until now, it might have been preferentially a freshwater
623 foraging area.

624 As regards to the empirical data, the observed variation and allometries in the skull bones,
625 mainly the PA, QJ, SQ, QU, PO, JU, MX, PAL and PT, as well as PCAs loadings, reflect shape
626 differences in both upper and lower adductor chambers. We interpret this allometric variation as
627 an indicative of more area attachment and resistance for stronger adductor muscles, which are
628 accompanied by changes in diet during aging, from softer to harder prey, as seen in living turles
629 species.

630 As regards to the use of images for carrying out morphometrics studies, we conclude that the use
631 of calipers can be replaced by softwares that work on images. ImageJ is an useful and time-
632 saving tool for this matter. However, one needs to beware when measuring straight lines between
633 landmarks that are located in different depths, which result in angled lines against the projection
634 orthogonal plane. Unattention to this detail will lead to assess lower values for a given
635 measurement than its real size.

636 Regarding the approaches applied to our data to deal with missing entries in the matrix (i.e. mean
637 value or iterative imputation), both were useful for answering the questions we raised (i.e. the
638 single population hypothesis), though little different results were obtained (few specimens out of
639 95% confidence ellipse in mean value approach in contrast with none specimen out of ellipse in
640 iterative imputation approach). However, we recommend the iterative imputation as the most

appropriate approach to deal with missing data in paleontological studies on the basis of the statistical assumptions it was developed (a sample-based regression for characters estimation) and the more conservative results.

Institutional Abbreviations: AMNH – American Museum of Natural History, New York, NY, United States; **LPRP –** Laboratório de Paleontologia da Faculdade de Filosofia, Ciências e Letras de Ribeirão Preto, Universidade de São Paulo, Ribeirão Preto, SP, Brazil; **MN –** Museu Nacional, Universidade Federal do Rio de Janeiro, Rio de Janeiro, RJ, Brazil; **MCT –** Museu de Ciências da Terra, Departamento Nacional de Produção Mineral, Rio de Janeiro, RJ, Brazil; **MCZ –** Museum of Comparative Zoology, Harvard University, Cambridge, MA, United States; **MZSP -** Museu de Zoologia, Universidade de São Paulo, São Paulo, SP, Brazil.

Anatomical abbreviations: PF – prefrontal; **FR –** frontal; **PA –** parietal; **VO –** vomer; **PAL –** palatine; **PT –** pterygoid; **BS –** basisphenoid; **BO –** basioccipital; **MX –** maxilla; **JU –** jugal; **QJ –** quadratojugal; **QU –** quadrate; **PO –** postorbital; **SQ –** squamosal; **OP –** opisthotic; **CO –** choanal.

Measurements abbreviations: TLS – Total length of skull; **LPF –** Length of prefrontal; **LFR –** Length of frontal; **LPA –** Length of parietal; **LVO –** Length of vomer; **LPAL –** Length of palatine; **LPT –** Length of pterygoid; **LBS –** Length of basisphenoid; **LBO –** Length of basioccipital; **LMX –** Length of maxilla; **LJU –** Length of jugal; **LQJ –** Length of quadratojugal; **LQU –** Length of quadrate; **LPO –** Length of postorbital; **LSQ –** Length of squamosal; **TWS –** Total width of skull; **WPF –** Width of prefrontal; **WFR –** Width of frontal; **WPA –** Width of parietal; **SMX –** Stretch of maxilla; **WVO –** Width of vomer; **WCO –** Width of choanal; **WPAL –** Width of palatine; **WBS –** Width of basisphenoid; **WMX –** Width of

maxilla; **WJU –** Width of jugal; **WQJ –** Width of quadratojugal; **WPO –** Width of postorbital; **WOP –** Width of opisthotic.

Acknowledgments

We are grateful to Sergio Azevedo, Deise Henriques, Luciana Carvalho, Lílian Cruz (DGP/MN) and Max Langer (LPRP/USP) for they allowed the loan of the material and visits to collections when necessary. Pedro Romanothanks the following people and institutions for facilitating access to collections: E. Gaffney, C. Mehling and F. Ippolito (AMNH); R. Cassab and R. Machado (MCT). We thank to Gustavo Oliveira (UFRPE) for being part of Thiago Mariani undergraduate thesiscommittee and for making revisions, suggestions, and comments that contributed to this paper; and to M. Lambertz (University of Bonn) and C. Mariani for revisions and comments on early versions of the manuscript. Torsten Scheyer and a second annonymous reviewer provided comments and insights that greatly improved the manuscript. Preliminary results of this paper composed the undergraduate thesis of Thiago Mariani.

6. References

AERTS P, VAN DAMME J, HERREL A. 2001. Intrinsic mechanics and control of fast cranio-cervical movements in aquatic feeding turtles. American Zoologist 41:1299-1310. DOI: dx.doi.org/10.1668/0003-1569(2001)041[1299:IMACOF]2.0.CO;2.

AGUILERA OA. 2004. Tesoros Paleontológicos de Venezuela. Urumaco, Patrimonio Natural de la Humanidad. Editorial Arte: Caracas.

ANQUETIN J. 2012. Reassessment of the phylogenetic interrelationships of basal turtles (Testudinata). Journal of Systematic Paleontology 10(1):3-45. DOI: 10.1080/14772019.2011.558928.

ASTUA D. 2009. Evolution of scapula size and shape in didelphid marsupials (Didelphimorphia: Didelphidae). Evolution 63(9): 2438-2456. DOI: 10.1111/j.1558-5646.2009.00720.x.

BAILEY SE. 2004. A morphometric analysis of maxillary molar crowns of Middle-Late Pleistocene hominins. Journal of Human Evolution 47(3): 183-198. DOI: dx.doi.org/10.1016/j.jhevol.2004.07.001.

BERTINI RJ, SANTUCCI RM, TOLEDO CEV, MENEGAZZO MC. 2006. Taphonomy and depositional history of an Upper Cretaceous turtle-bearing outcrop from the Adamantina Formation, Southwestern São Paulo state. Revista Brasileira de Paleontologia 9(2):181-186.

BHULLAR BAS, MARUGÁN-LOBÓN J, RACIMO F, BEVER GS, ROWE TB, NORELL MA, ABZHANOV A. 2012. Birds have paedomorphic dinosaur skulls. Nature 0. DOI: 10.1038/nature11146.

BURNELL A, COLLINS S, YOUNG BA. 2012. Vertebral morphometrics in *Varanus.* Bulletin de la Societe Geologique de France 183(2): 151-158.

CADENA EA, BLOCH JI, JARAMILLO CA. 2010. New podocnemidid turtle (Testudines: Pleurodira) from the Middle-Upper Paleocene of South America. Journal of Vertebrate Paleontology 30(2):367-382. DOI: dx.doi.org/10.1080/02724631003621946.

CADENA EA, BLOCH JI, JARAMILLO CA. 2012. New bothremydid turtle (Testudines, Pleurodira) from the Paleocene of Northeastern Colombia. Journal of Paleontology 86(4):688-698. DOI: dx.doi.org/10.1666/11-128R1.1.

CADENA EA, KSEPKA DT, JARAMILLO CA, BLOCH JI. 2012. New pelomedusoid turtles from the late Paleocene Cerrejón Formation of Colombia and their implications for phylogeny and body size evolution. Journal of Systematic Paleontology 10(2):313-331. DOI: dx.doi.org/10.1080/14772019.2011.569031.

CAMPOS DA, OLIVEIRA GR, FIGUEIREDO RG, RIFF D, AZEVEDO SAK, CARVALHO LB, KELLNER AWA. 2011. On a new peirosaurid crocodyliform from the Upper Cretaceous, Bauru Group, southeastern Brazil. Anais da Academia Brasileira de Ciências 83(1):317-327. DOI: dx.doi.org/10.1590/S0001-37652011000100020.

CLAUDE J, PRITCHARD PCH, TONG H, PARADIS E, AUFFRAY JC. 2004. Ecological correlates and evolutionary divergence in the skull of turtles: a geometric mophometric assessment. Systematic Biology 53(6):933-962. DOI: 10.1080/10635150490889498.

CONGDON JD, NAGLE RD, KINNEY OM, SELS RCVL, QUINTER T, TINKLE DW. 2003. Testing hypotheses of aging in long-lived painted turtles (Chrysemys picta). Experimental Gerontology 38:765-772.

COSTA HC, MOURA MR, FEIO RN. 2013. Taxonomic revision of *Drymoluber* Amaral, 1930 (Serpentes: Colubridae). Zootaxa 3716(3): 349-394. DOI: dx.doi.org/10.11646/zootaxa.3716.3.3.

DALRYMPLE GH. 1977. Intraspecific variation in the cranial feeding mechanism of turtles of the genus *Trionyx* (Reptilia, Testudines, Trionychidae). Journal of Herpetology 11(3):255-285. DOI: 10.2307/1563241.

DEPECKER M, RENOUS S, PENIN X, BERGE C. 2005. Procrustes analysis: a tool to understand shape changes of the humerus in turtles (Chelonii). Comptes Rendus Palevol 5: 509-518.

DEPECKER M, BERGE C, PENIN X, RENOUS S. 2006. Geometric morphometrics of the shoulder girdle in extant turtles (Chelonii). Journal of Anatomy 208: 35-45.

DE BROIN F. 1991. Fossil turtles from Bolivia. In: Suarez-Soruco R. *Fossiles y facies de Bolívia – Vol. I Vertebrados*. Revista Técnica de YPFB, 12(3-4): 509-527.

DE LA FUENTE MS, STERLI J, MANIEL I. 2014. Origin, evolution and biogeographic history of South American turtles. Springer Earth System Sciences.

FABRE AC, CORNETTE R, PERRARD A, BOYER DM, PRASAD GR, HOOKER JJ, GOSWAMI A. 2014. A three-dimensional morphometric analysis of the locomotory ecology of *Deccanolestes*, a eutherian mammal from the Late Cretaceous of India. Journal of Vertebrate Paleontology 34(1): 146-156.

FERNANDES LB, COIMBRA AM. 2000. Revisão estratigráfica da parte oriental da Bacia Bauru (Neocretáceo). Revista Brasileira de Geociências 30(4):717-728.

FERREIRA GS, RINCÓN AD, SOLÓRZANO A, LANGER MC. 2015. The last marine pelomedusoids (Testudines: Pleurodira): a new species of *Bairdemys* and the paleoecology of Stereogyina. PeerJ 3:e1063. DOI: 10.7717/peerj.1063.

FRANÇA MAG, LANGER MC. 2005. A new freshwater turtle (Reptilia, Pleurodira, Podocnemidae) from the Upper Cretaceous (Maastrichtian) of Minas Gerais, Brazil. Geodiversitas 27: 391-411.

FRAZZETTA TH. 1968. Adaptative problems and possibilities in the temporal fenestration of tetrapod skulls. Journal of Morphology 125:145-157.

FULFARO VJ, PERINOTTO JAJ. 1996. A Bacia Bauru: estado da arte. Boletim do Quarto Simpósio sobre o Cretáceo do Brasil, UNESP, Rio Claro, SP: 297-303.

FUTUYMA DJ. 1993. *Biologia evolutiva*. 2 ed. Ribeirão Preto: FUNPEC-RP.

GAFFNEY ES. 1972. An Illustred Glossary of Turtle Skull Nomeclature. American Museum Novitates 2486:33pp.

751 GAFFNEY ES. 1975. A phylogeny and classification of the higher categories of turtles. Bulletin
752 of the Americam Museum of Natural History 155(5):387-436.

753 GAFFNEY ES. 1979. Comparative Cranial Morphology of Recent and Fossil Turtles. Bulletin of
754 the American Museum of Natural History 164(2):65-376.

755 GAFFNEY ES, MEYLAN PA, WOOD RC, SIMONS E, CAMPOS DA. 2011. Evolution of the
756 side-necked turtles: the family Podcnemididae. Bulletin of the American Museum of Natural
757 History 350: 237pp. DOI: dx.doi.org/10.1206/350.1.

758 GAFFNEY ES., MEYLAN PA, WYSS AR. 1991. A computer assisted analysis of the
759 relationships of the higher categories of turtles. Cladistics 7:313-335. DOI: 10.1111/j.1096-
760 0031.1991.tb00041.x.

761 GAFFNEY ES, SCHEYER TM, JOHNSON KG, BOCQUENTIN J, AGUILERA OA. 2008.
762 Two new species of the side necked turtle genus, *Bairdemys* (Pleurodira, Podocnemididae), from
763 the Miocene of Venezuela. Palaontoloqische Zeitschrift 82(2):209-229.

764 GAFFNEY ES, TONG H, MEYLAN PA. 2006. Evolution of the sidenecked turtles: the families
765 Bothremydidae, Euraxemydidae and Araripemydidae. Bulletin of the American Museum of
766 Natural History 300:698pp. DOI: dx.doi.org/10.1206/0003-
767 0090(2006)300[1:EOTSTT]2.0.CO;2.

768 GOULD SJ. 1966. Allometry and size in ontogeny and phylogeny. Biological Reviews 41:587-
769 640. DOI: 10.1111/j.1469-185X.1966.tb01624.x.

770 GOULD SJ. 1979. An allometric interpretation of species-area curver: the meaning of the
771 coefficient. The American Naturalist 114(3):335-343.

772 HAMMER Ø, HARPER DAT, RYAN PD. 2001. Past: Palentological Statistics software
773 package for education and data analysis. Palaeontologia Electronica 4(1):9pp.

774 HAMMER Ø, HARPER DAT. 2006. *Paleontological Data Analysis*. Blackwell.

775 HENNIG, W. 1966. *Phylogenetic Systematics*. Urbana: University of Illinois Press.

776 HENRIQUES DDR. 2006. Sítio fossilífero de Pirapozinho: estudo de aspectos taxonômicos
777 através da análise básica e do exame de tomografia computadorizada. D. Phil. Thesis. Museu
778 Nacional – Universidade Federal do Rio de Janeiro.

779 HENRIQUES DDR, SUÁREZ JM, AZEVEDO SAK, CAPILLA R, CARVALHO LB. 2002. A
780 brief note on the paleofauna of "Tartaruguito" site, Adamantina Formation, Bauru Group, Brazil.
781 Anais da Academia Brasileira de Ciências 74(2): 366.

HENRIQUES DDR, AZEVEDO SAK, CAPILLA R. SUÁREZ JM. 2005. The Pirapozinho Site – a taphofacies study. Journal of Vertebrate Paleontology 25:69A.

HERREL A, O'REILLY JC, RICHMOND AM. 2002. Evolution of bite performance in turtles. Journal of Evolutionary Biology 15:1083-1094. DOI: 10.1046/j.1420-9101.2002.00459.x.

HUXLEY JS. 1950. Relative growth and form transformation. Proceedings of the Royal Society of London B 137:465-469. DOI: 10.1098/rspb.1950.0055.

HUXLEY JS, TEISSIER G. 1936. Terminology of Relative Growth. Nature 137:780-781. DOI: 10.1038/137780b0.

ILIN A, RAIKO T. 2010. Practical approaches to Principal Components Analysis in the presence of missing values. Journal of Machine Learning Research 11:1957-2000.

JARAMILLO CA, BAYONA G, PARDO-TRUJILLO A, RUEDA M, TORRES V, HARRINGTON GJ, MORA G. 2007. The palynology of the Cerrejón formation (Upper Paleocene) of northern Colombia. Palynology 31(1):153-189. DOI: 10.1080/01916122.2007.9989641.

JOLICOEUR P, MOSIMANN JE. 1960. Size and shape variation in the painted turtle: a Principal Component Analysis. Growth 24: 339-354.

JONES MEH, WERNEBURG I, CURTIS N, PENROSE R, O'HIGGINS P, FAGAN MJ, EVANS SE. 2012. The head and neck anatomy of sea turtles (Cryptodira: Chelonioidea) and skull shape in Testudines. PloS ONE 7(11):e47852. DOI: 10.1371/journal.pone.0047852. DOI: 10.1371/journal.pone.0047852.

JOYCE WG. 2007. Phylogenetic relationships of Mesozoic turtles. Bulletin of Peabody Museum of Natural History 48(1):3-102. DOI: dx.doi.org/10.3374/0079-032X(2007)48[3:PROMT]2.0.CO;2.

JOYCE WG, LYSON TR. 2010. A neglected lineage of north american turtles fills a major gap in the fossil record. Paleontology 53(2): 241-248. DOI: 10.1111/j.1475-4983.2009.00929.x

KISCHLAT EE. 1994. Observações sobre *Podocnemis elegans* Suaréz (Chelonii, Pleurodira, Podocnemididae) do Neocretáceo do Brasil. Acta Geologica Leopoldensia, 39: 345-351.

KISCHLAT EE, BARBARENA, MC, TIMM, LL. 1994. Considerações sobre a queloniofauna do Grupo Bauru, Neocretáceo do Brasil [Boletim do Simpósio sobre o Cretáceo do Brasil, Rio Claro: Universidade Estadual Paulista. 105-107.

KLINGER RC, MUSICK JA. 1995. Age and growth of loggerhead turtles (*Caretta caretta*) from Chesapeake Bay. Copeia 1:204-209.

KRZANOWSKI WJ. 1979. Between-Groups comparison of Principal Components. Journal of the American Statistical Association 74: 703-707.

KRZANOWSKI WJ. 1979. Between-Groups comparison of Principal Components – some sampling results. Journal of Statistical Computation Simulation 15: 141-154.

LEMELL P, BEISSER CJ, WEISGRAM J. 2000. Morphology and function of the feeding apparatus of *Pelusios castaneus* (Chelonia; Pleurodira). Journal of Morphology 244:127-135. DOI: 10.1002/(SICI)1097-4687(200005)244:2<127::AID-JMOR3>3.0.CO;2-U.

LEMELL P, LEMELL C, SNELDERWAARD P, GUMPENBERGER M, WOCHESLÄNDER R, WEISGRAM J. 2002. Feeding patterns in *Chelus fimbriatus* (Pleurodira: Chelidae). The Journal of Experimental Biology 205:1495-1506. PubMed: 11976360.

LYSON TR, JOYCE WG. 2009. A new species of *Palatobaena* (Testudines: Baenidae) and a maximum parsimony and bayesian phylogenetic analysis of Baenidae. Journal of Paleontology 83(3): 457-470. DOI: dx.doi.org/10.1666/08-172.1.

MARIANI TF, ROMANO PSR. 2014. Quando não podemos usar paquímetro: ImageJ como ferramenta para obtenção de dados morfométricos em fósseis [abstract no. 61]. Boletim de Resumos do IX Simpósio Brasileiro de Paleontologia de Vertebrados.

MALVASIO A, SOUZA AM., MOLINA FB, SAMPAIO FA. 2003. Comportamento e preferência alimentar em *Podocnemis expansa* (Schweigger), *P. unifilis* (Troschel) e *P. sextubeculata* (Cornalia) em cativeiro (Testudines, Pelomedusidae). Revista Brasileira de Zoologia, 20(1):161-168. DOI: dx.doi.org/10.1590/S0101-81752003000100021.

MINGOTI SA. 2013. Análise de dados através de métodos de estatística multivariada: uma abordagem aplicada. Editora UFMG.

MURPHY EC, HOGANSON J, JOHNSON K. 2003. Lithostratigraphy of the Hell Creek Formation of North Dakota. In: Hartman JH, Johnson KR, and Nichols DJ ed, *The Hell Creek Formation and Cretaceous-Tertiary Boundary in the Great Plains: An Integrated Continental Record of the End of the Cretaceous*. The Geological Society of America, Special Paper 361. 9–34.

NORELL MA, WHEELER WC. 2003. Missing entry replacement data analysis: a replacement approach to dealing with missing data in paleontological and total evidence data sets. Journal of Vertebrate Paleontology 23(2): 275-283.

OLIVEIRA GR. 2011. Filogenia e descrição de novos Podocnemididae (Pleurodira: Pelomedusoides). D. Phil. Thesis. Museu Nacional – Universidade Federal do Rio de Janeiro.

OLIVEIRA GR, ROMANO PSR. 2007. Histórico dos achados de tartarugas fósseis do Brasil. Arquivos do Museu Nacional 65(1):113-133.

PARSONS TS, WILLIAMS EE. 1961. Two Jurassic turtle skulls: a morphological study. Bulletin of the Museum of Comparative Zoology 125(3):41-107.

PERES-NETO PR, JACKSON DA, SOMERS KM. 2003. Giving meaningful interpretation to ordination axes: assessing loading significance in Principal Component Analysis. Ecology 84(9): 2347-2363.

PFALLER JB, GIGNAC PM, ERICKSON GM. 2011. Ontogenetic changes in jaw-muscle architecture facilitate durophagy in turtle *Sternotherus minor*. Journal of Experimental Biology 214:1655-1667. DOI: 10.1242/jeb.048090.

PFALLER JB, HERRERA ND, GIGNAC PM, ERICKSON GM. 2010. Ontogenetic scaling of cranial morphology and bite-force generation in the loggerhead musk turtle. Journal of Zoology 280:280-289. DOI: 10.1111/j.1469-7998.2009.00660.x.

PRICE IL. 1953. Os quelônios da Formação Bauru, Cretáceo terrestre do Brasil meridional. Rio de Janeiro: Departamento Nacional de Produção Mineral/Divisão de Geologia e Mineralogia, 34pp. (Boletim 147).

RABI M, ZHOU CF, WINGS O, GE S, JOYCE WG. 2013. A new xinjiangchelyid turtle from the Middle Jurassic of Xinjiang, China and the evolution of the basipterygoid process in Mesozoic turtles. BMC Evolutionary Biology 13:203. DOI: 10.1186/1471-2148-13-203.

RASBAND WS. 1997. ImageJ, U.S.National Institutes of Health, Bethesda, Maryland, USA. *Avaiable at* www.imagej.nih.gov/ij/. 1997-2012.

RIEPPEL O. 1993. Patterns of Diversity in the Reptilian Skull. In: Hanken J, Hall BK, *The Skull, Vol. 2: Patterns of Structural and Systematic Diversity*. Chicago: The University of Chicago Press, 344-390.

RIFF D, ROMANO PSR, OLIVEIRA GR, AGUILERA OA. 2010. Neogene crocodile and turtle fauna in northern South America. In: Hoorn C, Wesselingh FP ed. *Amazonia, Landscape and Species Evolution: A Look into the Past*. Wiley-Blackwell Publishing. 259-280.

ROMANO PSR. 2008. An unusual specimen of *Bauruemys elegans* and its implication for the taxonomy of the side-necked turtles from Bauru Basin (Upper Cretaceous of Brazil). Journal of Vertebrate Paleontology 28 (suppl. 3): 133A-134A.

ROMANO PSR. 2010. Evolução do crânio em Pelomedusoides (Testudines, Pleurodira). D. Phil. Thesis. Museu Nacional – Universidade Federal do Rio de Janeiro.

ROMANO PSR, AZEVEDO SAK. 2006. Are extant podocnemidid turtles relicts of a widespread Cretaceous ancestor? South American Journal of Herpetology 1(3):175-184. DOI: 10.2994/1808-9798(2006)1[175:AEPTRO]2.0.CO;2.

ROMANO PSR, AZEVEDO SAK. 2007. Morphometric analysis of the Upper Cretaceous brazilian side-necked turtle *Bauruemys elegans* (Suárez, 1969) (Pleurodira, Podocnemididae). Arquivos do Museu Nacional 65(4):395-402.

ROMANO PSR, GALLO V, RAMOS RRC, ANTONIOLI L. 2014. *Atolchelys lepida*, a new side-necked turtle from the Early Cretaceous of Brazil and the age of Crown-Pleurodira. Biology Letters 10: 20140290. DOI: 10.1098/rsbl.2014.0290.

ROMANO PSR, OLIVEIRA GR, AZEVEDO SAK, CAMPOS DA. 2009. Lumping the podocnemidid turtles species from Bauru Basin (Upper Cretaceous of Southeastern of Brazil) [abstract no. 38]. Gaffney Turtle Symposium Abstract Volume: 141-152.

ROMANO PSR, OLIVEIRA GR, AZEVEDO SAK, KELLNER AWA, CAMPOS DA. 2013. New information about Pelomedusoides (Testudines: Pleurodira) from the Cretaceous of Brazil. In: Brinkman D, Holroyd P, Gardner J, ed. *Morphology and evolution of turtles.* Vertebrate Paleobiology and Paleoanthropology Series. Dordrecht, The Netherlands: Springer, 261-275.

SÁNCHEZ-VILLAGRA MR, AGUILERA OA. 2006. Neogene Vertebrates from Urumaco, Falcón State, Venezuela: Diversity and Significance. Journal of Systematic Palaeontology 4(3):213-220. DOI: 10.1017/S1477201906001829.

SÁNCHEZ-VILLAGRA MR, WINKLER JD. 2006. Cranial variation in *Bairdemys* turtles (Podocnemididae: Miocene of the Caribbean region) and description of new material from Urumaco, Venezuela. Journal of Systematic Paleontology 4(3):241-253. DOI: 10.1017/S1477201906001891.

SCHUMACHER GH. 1973. The head muscles and hyolaryngeal skeleton of turtles and crocodilians. In: Gans C, *Biology of Reptilia, vol. 4: Morphology D*. London: Academic Press, 101-199.

SHINE RS, IVERSON JB. 1995. Patterns of survival, growth and maturation in turtles. Oikos 72(3):343-348. DOI: 10.2307/3546119.

SMITH KK. 1993. The form of the feeding apparatus in terrestrial vertebrates: studies of adaptation and constraint. In: Hanken J, Hall BK, *The Skull, Vol. 3:Functional and Evolutionary Mechanisms.* Chicago: The University of Chicago Press, 150-196.

SOARES PC, LANDIM PMB, FULFARO VJ, NETO AFS. 1980. Ensaio de caracterização estratigráfica do Cretáceo no estado de São Paulo: Grupo Bauru. Revista Brasileira de Geociências 10:177-185.

SOMERS KM. 1989. Allometry, Isometry and Shape in Principal Components Analysis. Systematic Zoology 38(2):169-173.

914 STERLI J, DE LA FUENTE MS. 2010. Anatomy of *Condorchelys antiqua* Sterli, 2008, and the
915 origin of the modern jaw closure mechanism in turtles. Journal of Vertebrate Paleontology
916 30(2):351-366. DOI: 10.1080/02724631003617597.

917 STERLI J, MÜLLER J, ANQUETIN J, HILGER A. 2010. The parabasisphenoid complex in
918 Mesozoic turtles and the evolution of the testudinate basicranium. Canadian Journal of Earth
919 Sciences 47:1337-1346. DOI: 10.2307/3546119.

920 STRAUSS RE, ATANASSOV MN, OLIVEIRA JA. 2003. Evaluation of the principal-
921 component and expectation-maximization methods for estimating missing data in morphometric
922 studies. Journal of Vertebrate Paleontology 23(2): 284-296.

923 SUÁREZ, JM. 1969a. Um nôvo quelônio fóssil da Formação Baurú [abstract no. 153].
924 Comunicações do Congresso Brasileiro de Geologia, Salvador: Boletim Especial, Salvador,
925 1:87-89.

926 SUÁREZ, JM. 1969b. Um quelônio da Formação Bauru. Boletim da Faculdade de Filosofia,
927 Ciências e Letras de Presidente Prudente 2:35-54.

928 SUÁREZ, JM. 1969c. Um quelônio da Formação Bauru [abstract no. 12]. Anais do Congresso
929 Brasileiro de Geologia, Salvador. 167-176.

930 SUÁREZ JM. 2002. Sítio fossilífero de Pirapozinho, SP – Extraordinário depósito de quelônios
931 do Cretáceo. In: Schobbenhaus C, Campos DA, Queiroz ET, Winge M, Berbert-Born M. *Sítio*
932 *geológicos e paleontológicos do Brasil*.

933 VAN DAMME J, AERTS P. 1997. Kinematics and functional morphology of aquatic feeding in
934 australian snake-necked turtles (Pleurodira; *Chelodina*). Journal of Morphology 233:113-125.
935 DOI: 10.1002/(SICI)1097-4687(199708)233:2<127::AID-JMOR4>3.0.CO;2-3.

936 WERNEBURG I. 2011. The cranial musculature of turtles. Palaentologia eletronica 14(2):99p;
937 palaeo-electronica.org/2011_2/254/index.html.

938 WERNEBURG I. 2012. Temporal bone arrangements in turtles: an overview. Journal of
939 Experimental Zoology 318:235-249. DOI: 10.1002/jez.b.22450.

940 WERNEBURG I. 2013. The tendinous framework in the temporal skull region of turtles and
941 considerations about its morphological implications in amniotes: a review. Zoological Science
942 30:141-153. DOI: 10.2108/zsj.30.141.

943 WERNEBURG I, WILSON LAB, PARR WCH, JOYCE WG. 2014. Evolution of neck vertebral
944 shape and neck retraction at the transition to Modern Turtles: an integrated geometric
945 morphometric approach. Systematic Biology 0(0): 1-18. DOI: 10.1093/sysbio/syu072.

946 WINGS O, RABI M, SCHNEIDER JW, SCHWERMANN L, SUN G, ZHOU CF, JOYCE WG.
947 2012. An enormous Jurassic turtle bone bed from the Turpan Basin of Xinjiang, China.
948 Naturwissenschaften 99:925-935. DOI: 10.1007/s00114-012-0974-5.

949

Figure 1

Fossil turtle localities in Bauru Basin

Lithostratigraphical map of the oriental part of the Bauru Basin showing the fossil turtle localities (municipalities). Turtle species are: **1.** *Cambaremys langertoni* (*incertae sedis*), *Pricemys caieira* and *Peiropemys mezzalirai*; **2.** *Roxochelys harrisi* (*nomem dubium*); **3.** *Bauruemys brasiliensis* (*nomem dubium*) and Testudines indet.; **4.** Testudines indet.; **5.** Testudines indet.; **6.** *B. brasiliensis* and *Roxochelys wanderleyi*; **7.** Testudines indet.; **8.** Testudines indet.; **9.** Podocnemididae indet.; **10.** *Roxochelys* sp. and *R. wanderleyi*; **11.** *B. elegans*. Abbreviations: **GO,** Goiás State; **MG,** Minas Gerais State; **MS,** Mato Grosso do Sul State; **PR,** Paraná State; **SP,** São Paulo State. Scale bar in Km. Map modified from Romano et al. (2009); geology following Fernandes (2004); taxonomy status of species following Romano et al. (2013).

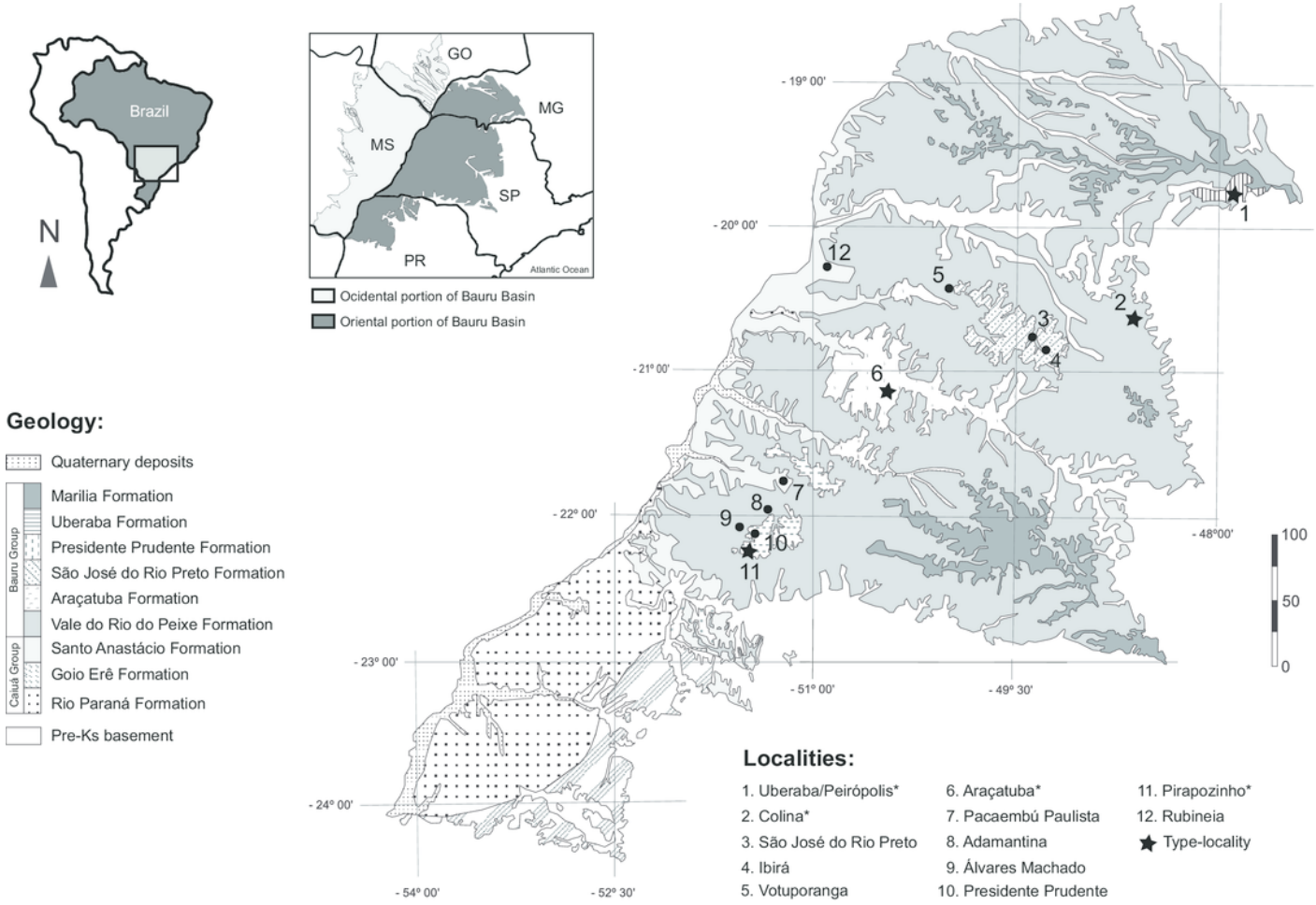
Brazil
N
GO
MG
MS
SP
PR
Atlantic Ocean
Ocidental portion of Bauru Basin
Oriental portion of Bauru Basin
Geology:
Quaternary deposits
Bauru Group
Marilia Formation
Uberaba Formation
Presidente Prudente Formation
São José do Rio Preto Formation
Araçatuba Formation
Vale do Rio do Peixe Formation
Caiuá Group
Santo Anastácio Formation
Goio Erê Formation
Rio Paraná Formation
Pre-Ks basement
- 19° 00'
- 20° 00'
- 21° 00'
- 22° 00'
- 23° 00'
- 24° 00'
- 54° 00'
- 52° 30'
- 51° 00'
- 49° 30'
- 48°00'
100
50
0
Localities:
1. Uberaba/Peirópolis*
2. Colina*
3. São José do Rio Preto
4. Ibirá
5. Votuporanga
6. Araçatuba*
7. Pacaembú Paulista
8. Adamantina
9. Álvares Machado
10. Presidente Prudente
11. Pirapozinho*
12. Rubineia
Type-locality

Figure 2

Image of landmarks used as references for taking measurements.

Skull of *Bauruemys elegans* in (A) dorsal, (B) ventral and (C) right lateral views showing the anatomical nomenclature and the 39 landmarks used for morphometrics analysis. All measurements were taken between two landmarks (see table 2 for vectors description). **Abbreviations: bo,** basioccipital; **bs,** basisphenoid; **ex,** exoccipital; **fpp,** foramen palatinum posterius; **fr,** frontal; **ju,** jugal; **mx,** maxilla; **op,** opisthotic; **pa,** parietal; **pal,** palatine; **pf,** prefrontal; **pm,** premaxilla; **po,** postorbital; **pt,** pterygoid; **ptp,** processus trochlearis pterygoidei; **qj,** quadratojugal; **qu,** quadrate; **sq,** squamosal; **so,** supraoccipital; **vo,** vomer. Skull lineation from Gaffney et al. (2011, p.72).

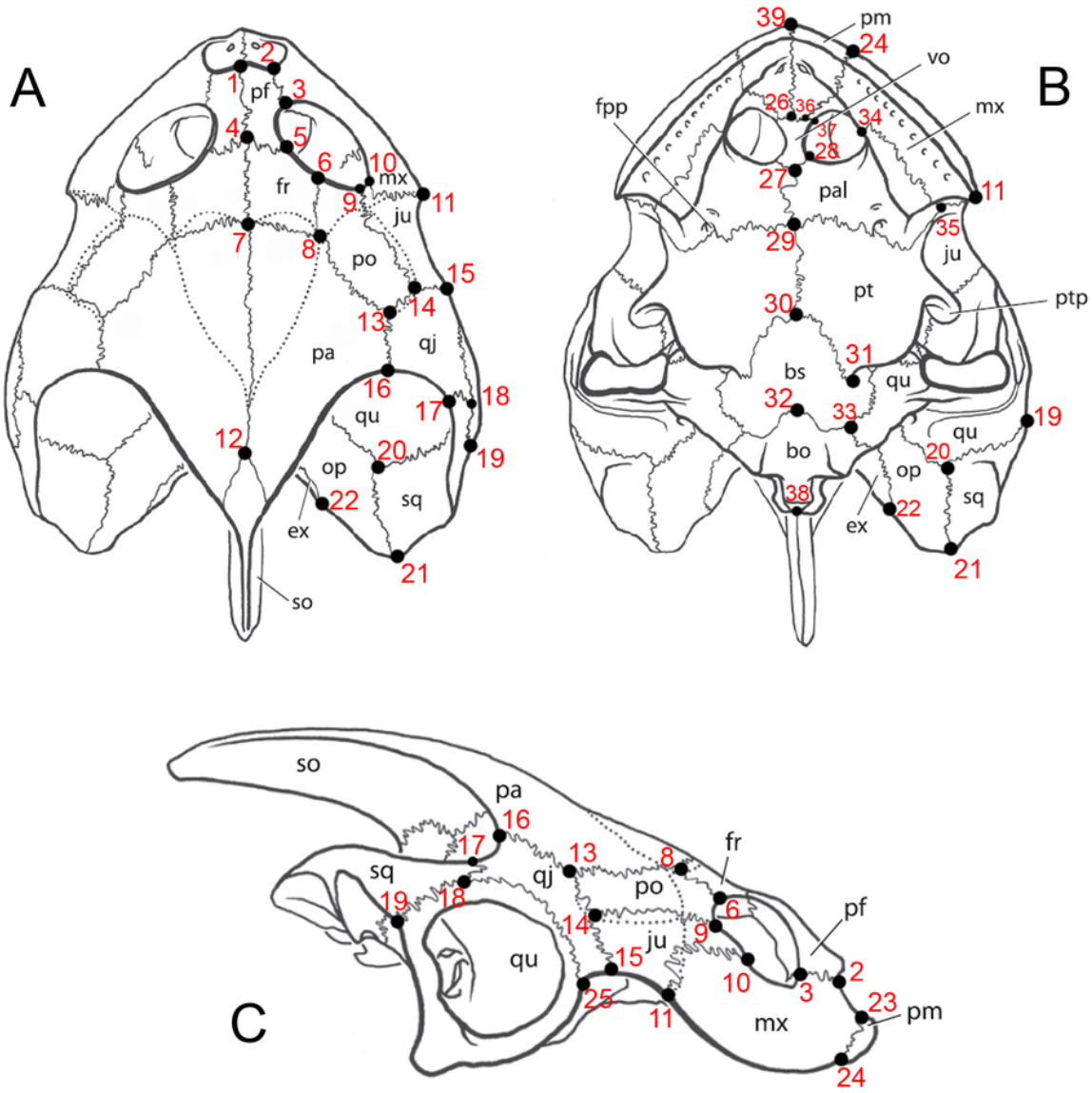
A
1
2
3
4
5
6
10
mx
fr
9
11
ju
7
8
po
15
14
13
qj
pa
16
18
17
qu
12
20
19
op
22
sq
ex
21
so
B
39
pm
24
vo
fpp
26
36
mx
34
37
28
27
pal
11
29
35
ju
pt
ptp
30
31
bs
qu
32
33
19
qu
bo
20
op
38
sq
ex
22
21
C
so
pa
16
17
13
8
fr
sq
qj
po
19
18
6
pf
14
9
ju
qu
15
10
2
25
3
23
pm
11
mx
24

Figure 3

Allometric graphics: part 1.

Allometries of *Bauruemys elegans* skull bones: (A) lenght of parietal (LPA), (B) lenght of maxilla (LMX), (C), lenght of jugal (LJU), (D) lenght of quadrate (LQU), (E) lenght of squamosal (LSQ), (F) lenght of pterygoid (LPT), (G) lenght of postorbital (LPO), (H) stretch of maxilla (SMX), (I) width of quadratojugal (WQJ) (J) and width of parietal (WPA). Angular coefficient (a) and coefficient of correlation (r) are shown. **Abbreviations: TLS,** total lenght of the skull; **TWS,** total width of the skull.

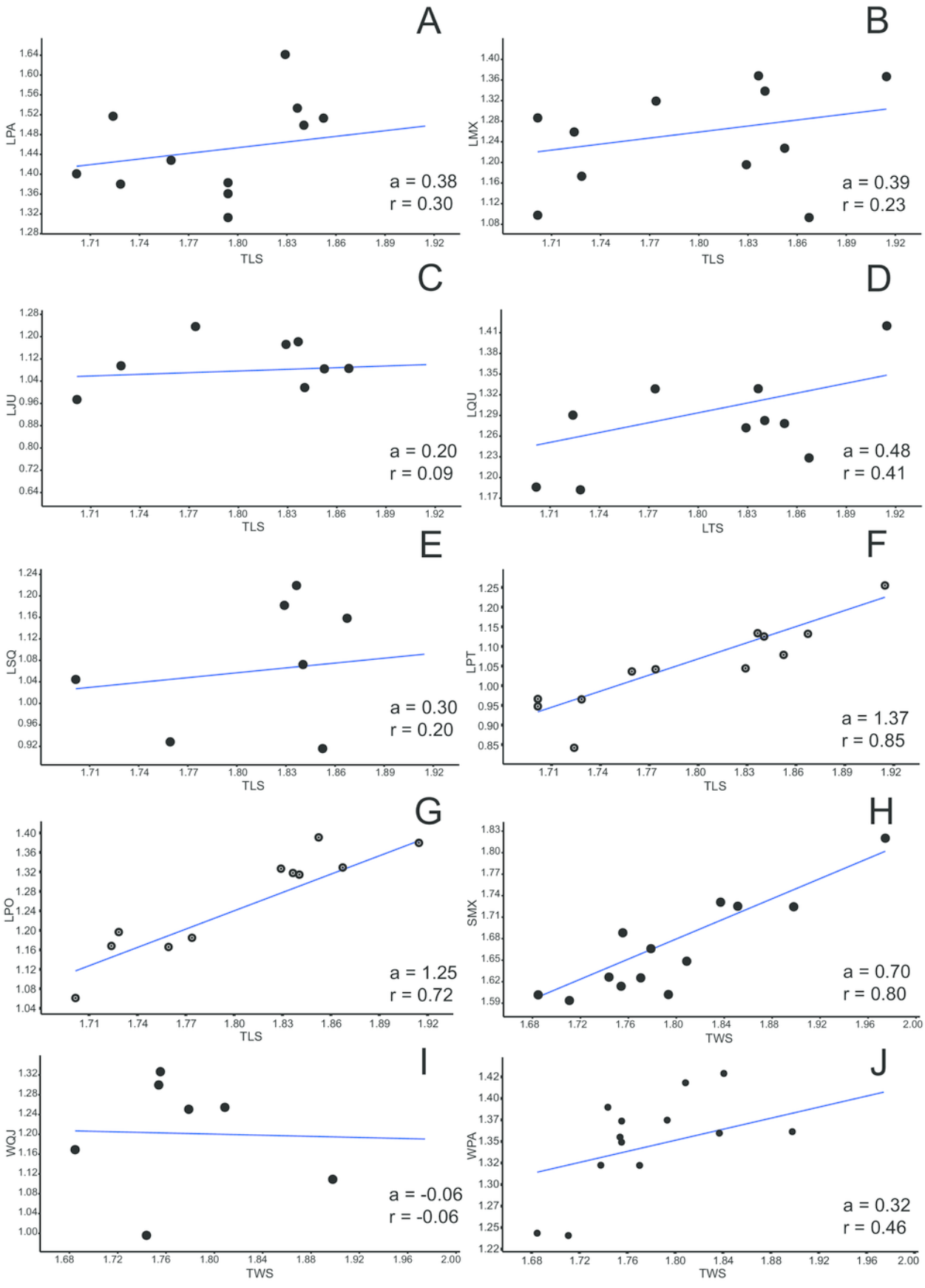
A
LPA
TLS
a = 0.38
r = 0.30
B
LMX
TLS
a = 0.39
r = 0.23
C
LJU
TLS
a = 0.20
r = 0.09
D
LQU
LTS
a = 0.48
r = 0.41
E
LSQ
TLS
a = 0.30
r = 0.20
F
LPT
TLS
a = 1.37
r = 0.85
G
LPO
TLS
a = 1.25
r = 0.72
H
SMX
TWS
a = 0.70
r = 0.80
I
WQJ
TWS
a = -0.06
r = -0.06
J
WPA
TWS
a = 0.32
r = 0.46

Figure 4

Allometric graphics: part 2.

Allometries of *Bauruemys elegans* skull bones: (A) lenght of basioccipital (LBO), (B) lenght of basisphenoid (LBS), (C), lenght of palatine (LPAL), (D) lenght of frontal (LFR), (E) lenght of prefrontal (LPF), (F) lenght of quadratojugal (LQJ), (G) lenght of vomer (LVO), (H) width of postorbital (WPO), (I) width of opisthotic (WOP) (J) and width of choanal (WCO). Angular coefficient (a) and coefficient of correlation (r) are shown. **Abbreviations: TLS,** total lenght of the skull; **TWS,** total width of the skull.

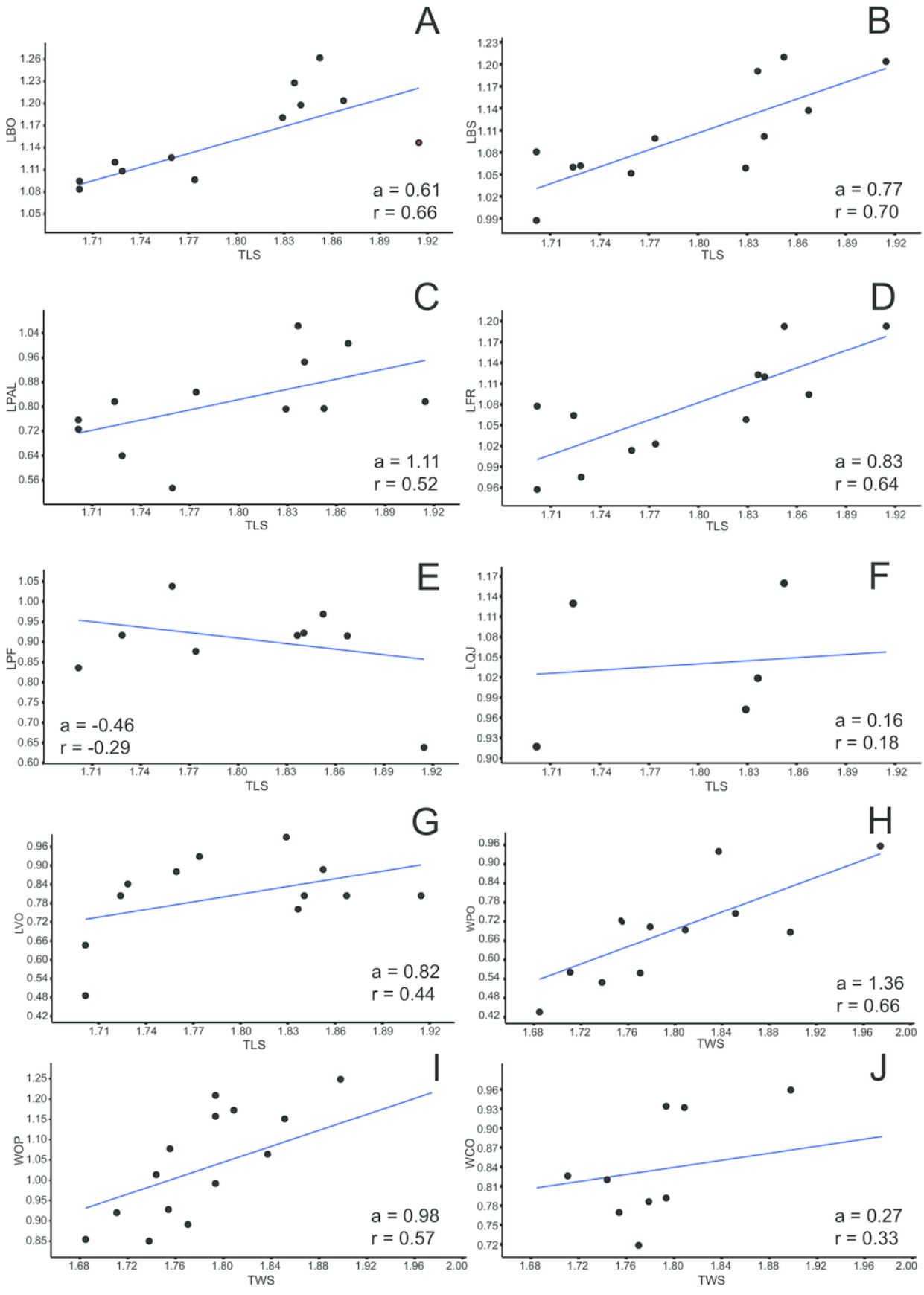
A
LBO
TLS
a = 0.61
r = 0.66
B
LBS
TLS
a = 0.77
r = 0.70
C
LPAL
TLS
a = 1.11
r = 0.52
D
LFR
TLS
a = 0.83
r = 0.64
E
LPF
TLS
a = -0.46
r = -0.29
F
LQJ
TLS
a = 0.16
r = 0.18
G
LVO
TLS
a = 0.82
r = 0.44
H
WPO
TWS
a = 1.36
r = 0.66
I
WOP
TWS
a = 0.98
r = 0.57
J
WCO
TWS
a = 0.27
r = 0.33

Figure 5

Allometric graphics: part 3.

Allometries of *Bauruemys elegans* skull bones: (A) width of maxilla (WMX), (B) width of jugal (WJU), (C), width of frontal (WFR), (D) width of prefrontal (WPF), (E) width of basisphenoid (WBS), (F) width of palatine (WPAL) and (G) width of vomer (WVO). Angular coefficient (a) and coefficient of correlation (r) are shown. **Abbreviations: TWS,** total width of the skull.

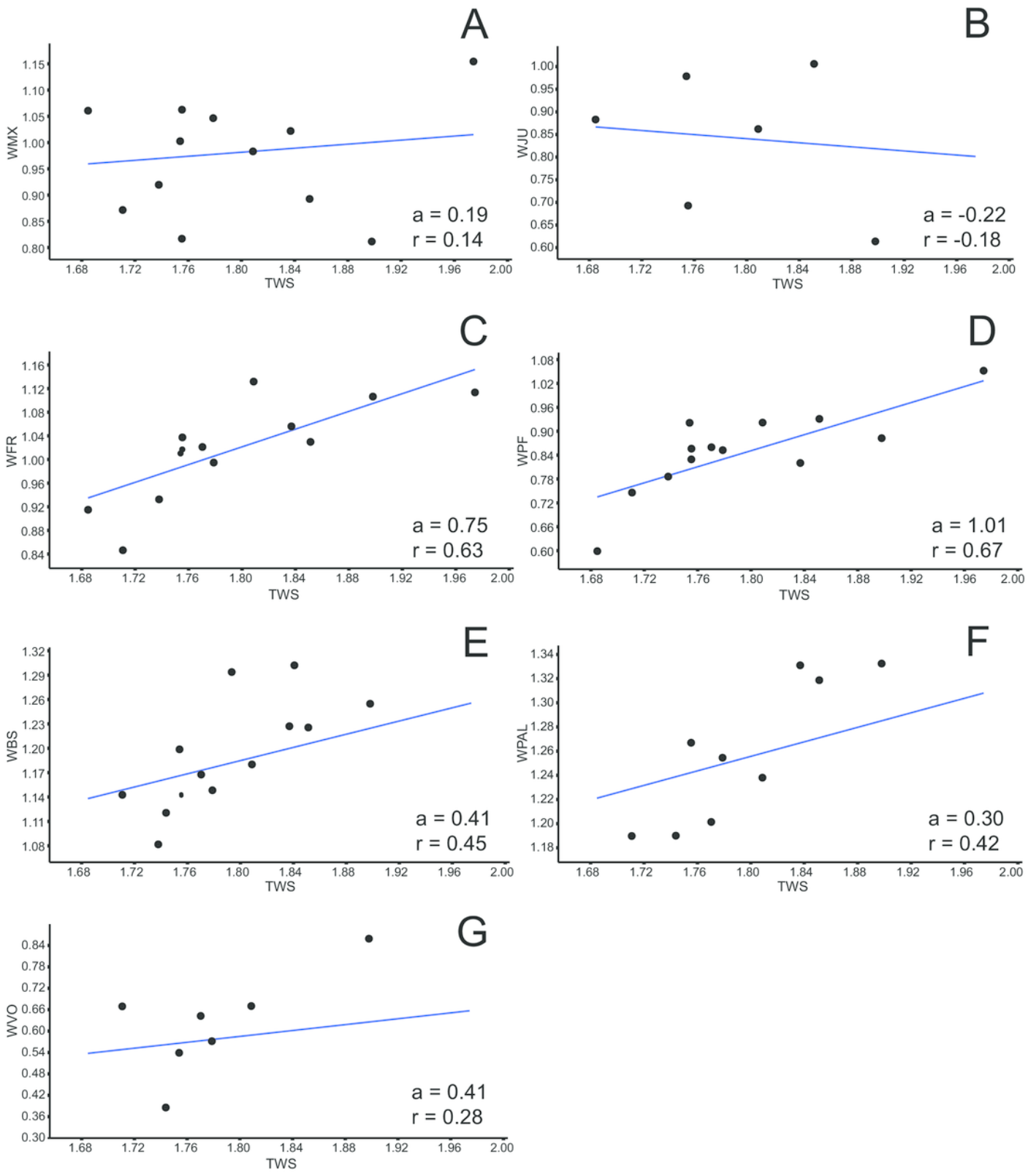
A
WMX
TWS
a = 0.19
r = 0.14
B
WJU
TWS
a = -0.22
r = -0.18
C
WFR
TWS
a = 0.75
r = 0.63
D
WPF
TWS
a = 1.01
r = 0.67
E
WBS
TWS
a = 0.41
r = 0.45
F
WPAL
TWS
a = 0.30
r = 0.42
G
WVO
TWS
a = 0.41
r = 0.28

Figure 6

PCA: raw data.

Principal Components Analysis (PCA) from raw data matrix using mean value substitution approach (A and B) and iterative imputation substitution approach (C) in replacing missing data. The 95% ellipse is given.

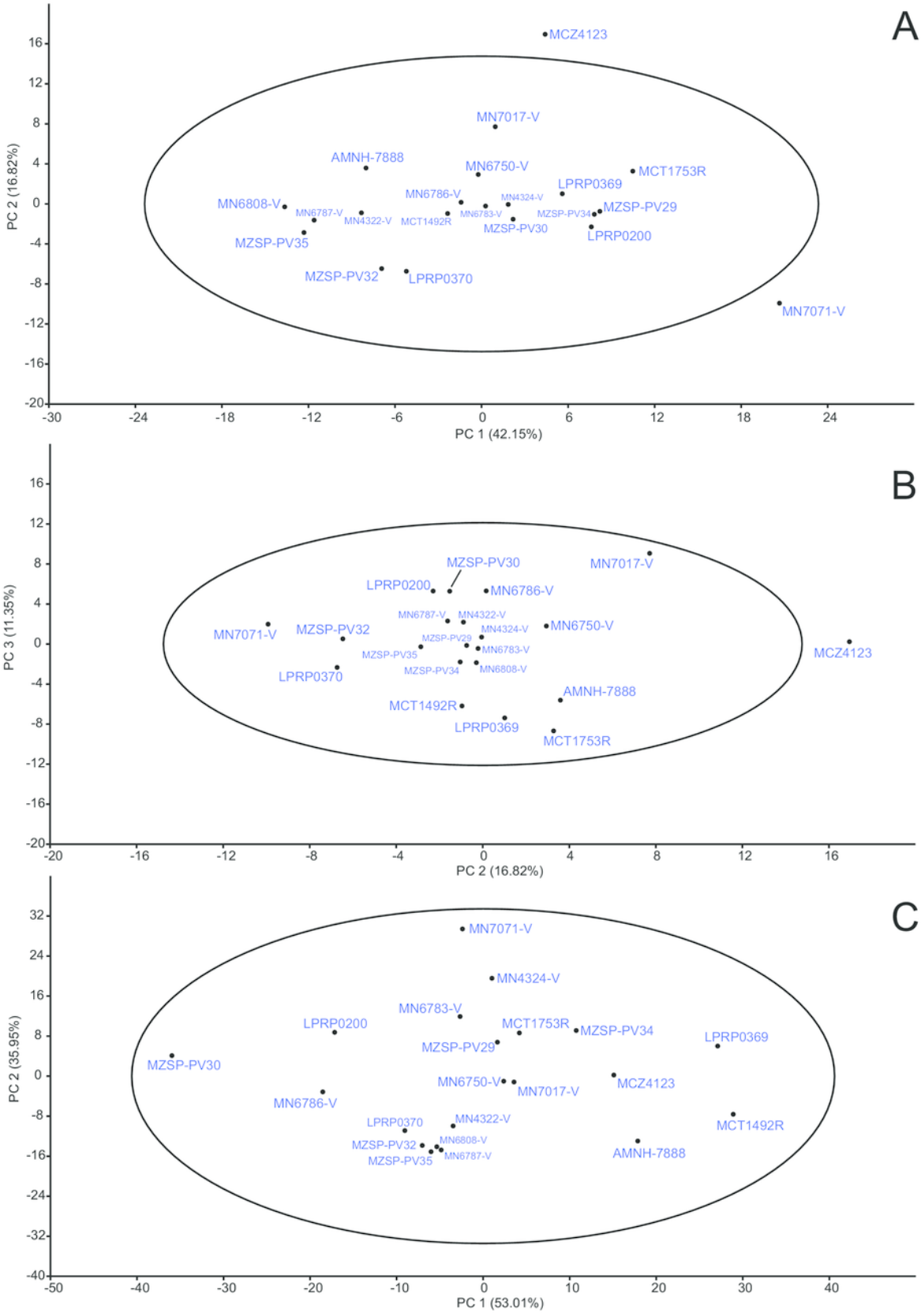
A
MCZ4123
MN7017-V
AMNH-7888
MN6750-V
MCT1753R
LPRP0369
MN6786-V
MN4324-V
MN6808-V
MN6787-V
MZSP-PV29
MN4322-V
MCT1492R
MN6783-V
MZSP-PV34
MZSP-PV30
LPRP0200
MZSP-PV35
MZSP-PV32
LPRP0370
MN7071-V
PC 2 (16.82%)
PC 1 (42.15%)
B
MZSP-PV30
MN7017-V
LPRP0200
MN6786-V
MN6787-V
MN4322-V
MN7071-V
MZSP-PV32
MN6750-V
MZSP-PV29
MN4324-V
MZSP-PV35
MN6783-V
MCZ4123
LPRP0370
MZSP-PV34
MN6808-V
AMNH-7888
MCT1492R
LPRP0369
MCT1753R
PC 3 (11.35%)
PC 2 (16.82%)
C
MN7071-V
MN4324-V
MN6783-V
LPRP0200
MCT1753R
MZSP-PV34
LPRP0369
MZSP-PV29
MZSP-PV30
MN6750-V
MCZ4123
MN7017-V
MN6786-V
LPRP0370
MN4322-V
MCT1492R
MZSP-PV32
MN6808-V
MZSP-PV35
MN6787-V
AMNH-7888
PC 2 (35.95%)
PC 1 (53.01%)

Figure 7

PCA: proportions data.

Principal Components Analysis (PCA) from proportions data matrix using mean value substitution approach (A) and iterative imputation substitution approach (B) in replacing missing data. The 95% ellipse is given.

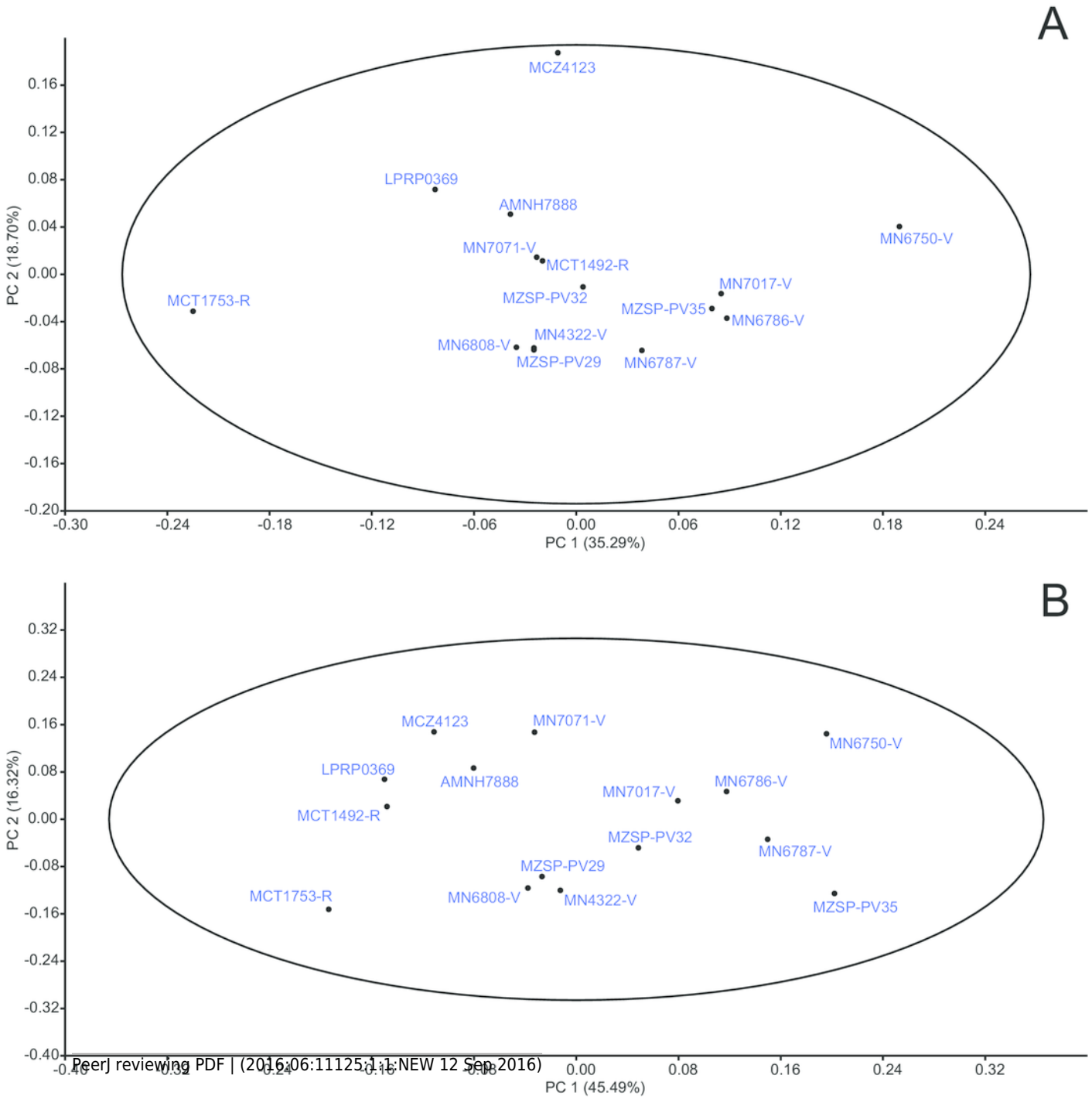

Figure 8

Comparison of a taphonomically altered skull with two well-preserved skulls of *Bauruemys elegans*, showing the cheek morphologies observed.

Bauruemys elegans specimens in dorsal view showing the largest MN7071-V specimen (A) in contrast with two smaller, well-preserved narrow-cheeked MN7017-V (B) and wide-cheeked MN4322-V (C) specimens. MN7071-V (A) is larger due to vertical crushing in the mediocaudal portion of the skull, resulting in artificial wide-cheeked morphology. In other specimens, such a taphonomic effect is not observed, indicating that both narrow- (B) and wide-cheeked (C) morphologies are naturally present in *B. elegans*.

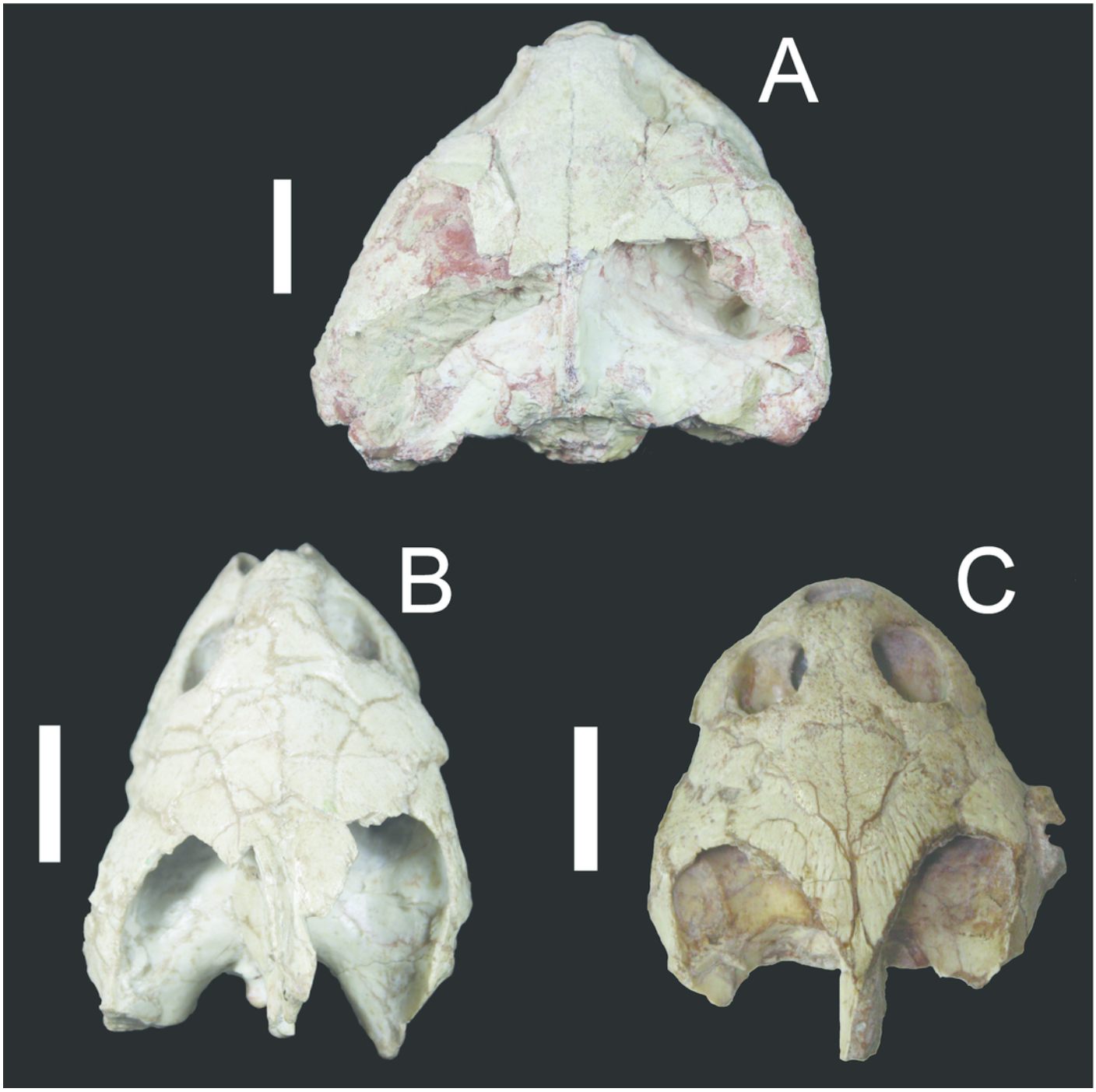
A
B
C

Figure 9

Evolution of PA-QJ contact and skull roofing in Podocnemidoidea.

Simplified phylogeny of Podocnemidoidea (Bothremydidae + Podocnemidinura) showing the evolution of the contact between parietal (green; PA) and quadratojugal (yellow; QJ), and its relation with the postorbital (red; PO) and skull roofing. Within Bothremydidae, both very emarginated (*Cearachelys placidoi*) and less emarginated (*Taphrosphys congolensis*) skulls are present, showing either no contact (*C. placidoi)* or contact present with small QJ (*T. congolensis*). Within Podocnemidinura, the contact PA-QJ is present and the skull roofing increased from a less roofed condition, found in *Brasilemys josai* and *Hamadachelys*, to a continuous increasingly growing well roofed condition within Podocnemididae, exemplified by *Bauruemys elegans*, *Lapparentemys vilavillensis* and *Podocnemis unifilis*, up to a fully roofed morphology in *Peltocephalus*. *Cearachelys placidoi* and *T. congolensis* modified from Gaffney et al. (2006); *Brasilemys josai* redrawn from Lapparent de Broin (2000); all others skulls modified from Gaffney et al. (2011).

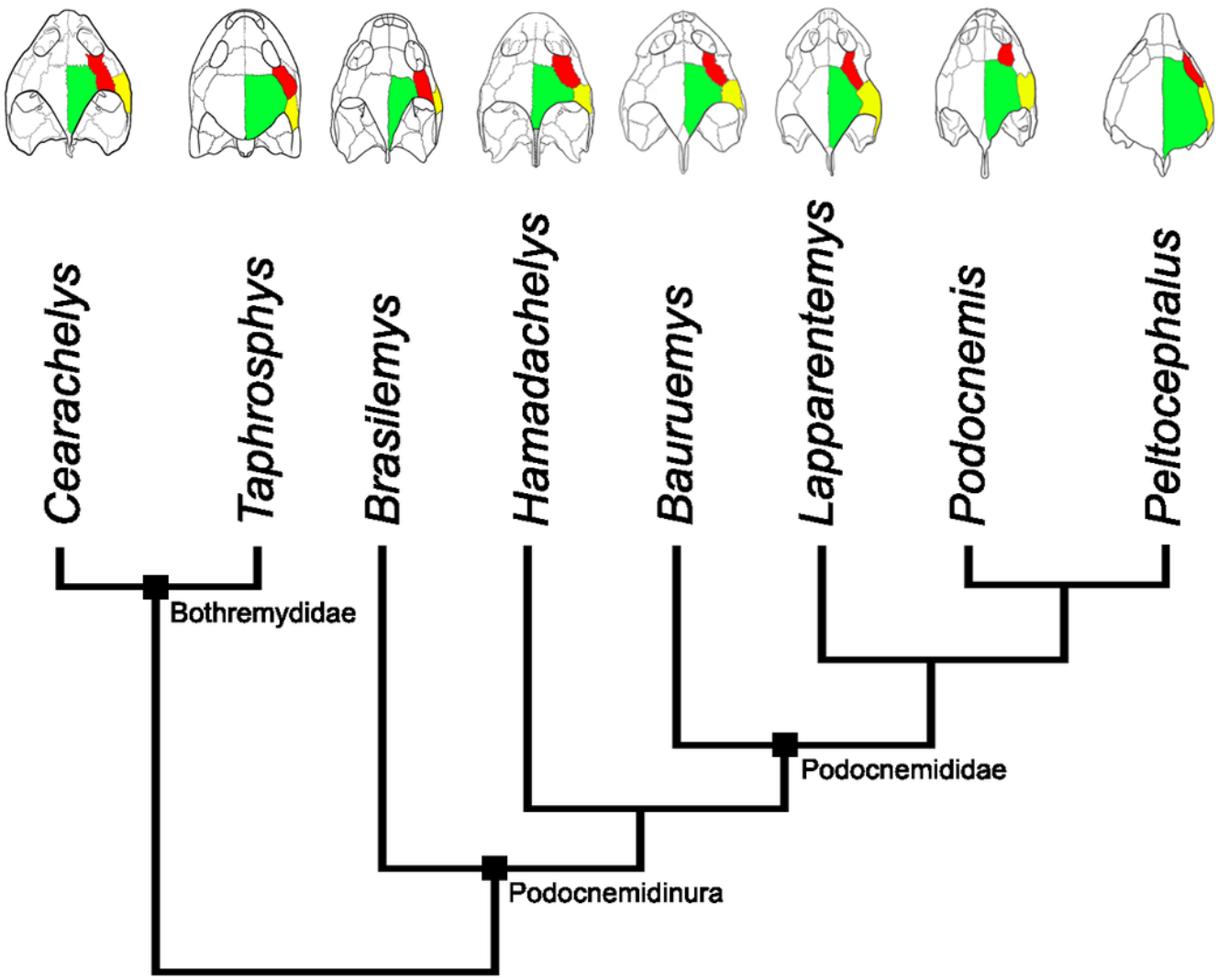
Cearachelys
Taphrosphys
Brasilemys
Hamadachelys
Bauruemys
Lapparentemys
Podocnemis
Peltocephalus
Bothremydidae
Podocnemididae
Podocnemidinura

Figure 10

Sketch of jaw-closing muscles and its vector forces in *Podocnemis expansa*.

Dorsal (A and C) and left lateral (B and D) view of the skull of *Podocnemis expansa* (MZSP-0038) showing the muscle attachment places (A and B) and the direction vector forces (C and D) during jaw closing. The muscles and vectors of *m. adductor mandibulae externus* (green), *m. adductor mandibulae posterior* (red), *m. pterygoideus* (blue), and *m. depressor mandibulae* (yellow) are sketched. Lenght and thickness of the arrows indicate the relative forces. **Abbreviations:** art, articular; **den,** dentary; **mx,** maxilla; **pa,** parietal; **ptp,** processus trochlearis pterygoidei; **qj,** quadratojugal; **qu,** quadrate; **so,** supraoccipital.

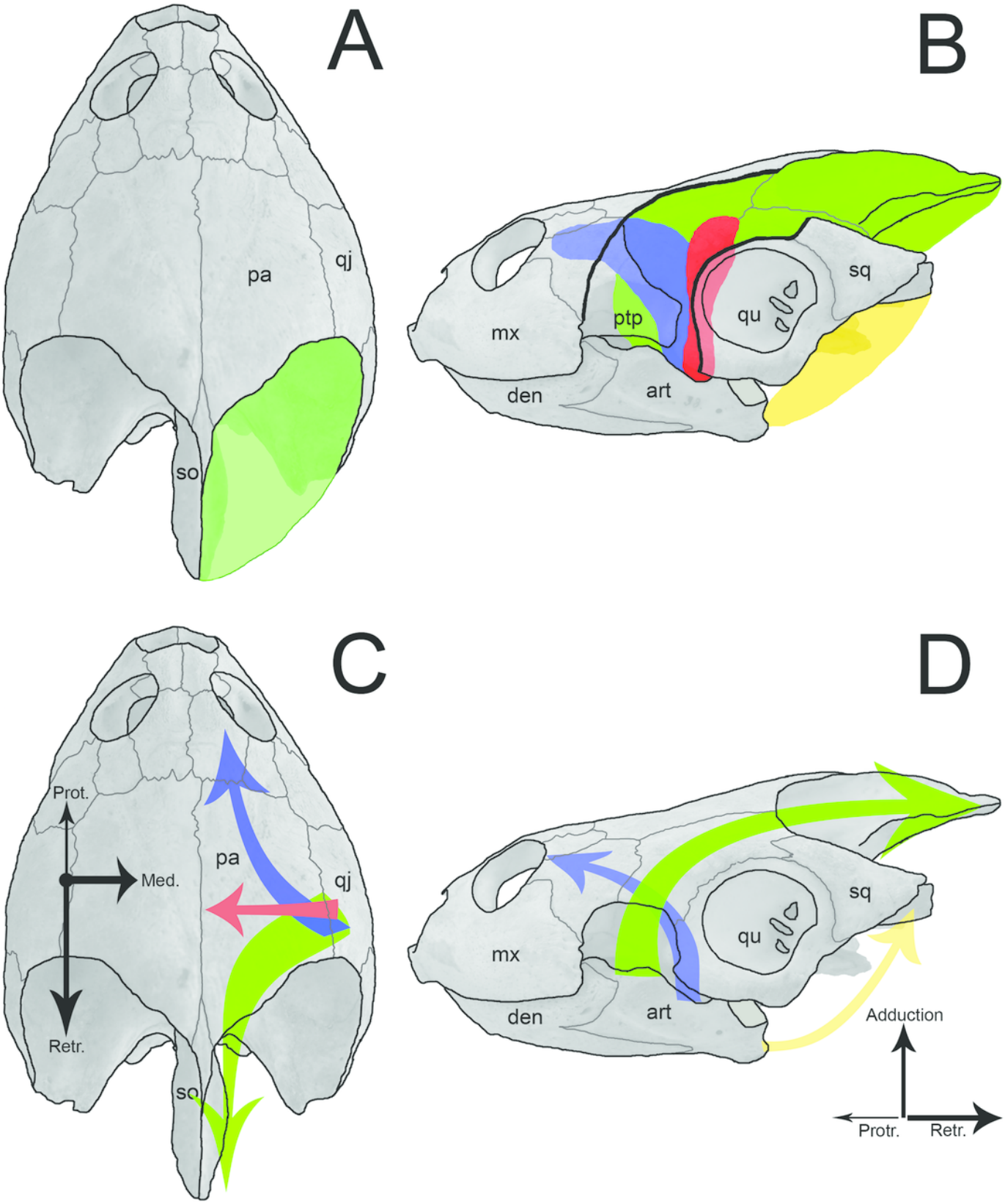
A
pa
qj
so
B
mx
ptp
qu
sq
den
art
C
Prot.
Med.
Retr.
pa
qj
so
D
mx
qu
sq
den
art
Adduction
Protr.
Retr.

Table 1(on next page)

ANOVA results for ImageJ and caliper comparisons.

Parameters calculated for each treatment of the ANOVA. The first three columns are relative to the caliper (cal). The three next are relative to the ImageJ (ImJ). The last column indicates the F values for each character. Measurements abbreviations: TLS, total lenght of the skull; TWS total width of the skull; LPF, lenght of prefrontal; WPF, width of prefrontal; LFR, lenght of frontal; WFR, width of frontal; LPA, lenght of parietal; WPA, width of parietal; SMX, stretch of maxilla; LVO, lenght of vomer; WVO, width of vomer; WCO, width of choannal; LPAL, lenght of palatine; WPAL, width of palatine; LPT, lenght of pterygoid; LBS, lenght of basisphenoid; WBS, width of basisphenoid; LBO, lenght of basisoccipital; LMX, lenght of maxilla; WMX, width of maxilla; LJU, lenght of jugal; WJU, width of jugal; LQJ, lenght of quadratojugal; WQJ, width of quadratojugal; LQU, lenght of quadrate; LPO, lenght of postorbital; WPO, width of postorbital; WOP, width of opisthotic; LSQ, lenght of squamosal.

Char.	N (Cal)	Mean (Cal)	σ (Cal)	N (ImJ)	Mean (ImJ)	σ (ImJ)	F value
TLS	8	63,72	10,87	8	62,26	11,36	0,069
TWS	9	60,42	9,45	8	64,83	13,58	0,617
LPF	9	9,78	1,26	9	8,05	1,80	5,617*
WPF	10	6,70	1,90	10	7,55	1,83	1,04
LFR	10	12,19	1,74	10	11,79	2,02	0,233
WFR	10	9,64	1,63	10	10,12	1,82	0,383
LPA	7	25,54	4,71	7	27,35	4,83	0,504
WPA	6	21,78	2,79	6	22,54	3,16	0,195
SMX	9	46,46	7,12	9	47,66	8,62	0,104
LVO	6	5,95	1,71	7	6,59	1,31	0,596
WVO	6	3,11	0,78	7	3,68	0,52	1,874
WCO	5	7,53	1,31	6	6,45	1,15	2,107
LPAL	7	8,26	1,25	8	7,21	2,81	0,828
WPAL	7	16,90	1,91	7	17,12	2,23	0,038
LPT	11	11,54	2,06	12	11,69	2,75	0,228
LBS	12	12,43	1,30	12	12,88	1,64	0,563
WBS	11	15,58	2,32	11	15,57	2,40	<0,001
LBO	7	13,00	1,84	7	13,84	1,85	0,726
LMX	10	24,28	4,20	9	19,22	4,15	6,937*
WMX	10	10,44	2,16	9	10,18	2,26	0,065
LJU	9	15,75	3,81	7	13,39	2,92	1,847
WJU	3	8,31	1,20	2	9,83	-**	2,709
LQJ	4	12,84	1,48	2	11,96	-**	0,366
WQJ	6	16,21	4,02	3	19,65	1,72	1,921
LQU	11	17,71	3,43	8	21,19	3,88	4,253
LPO	9	16,57	3,30	9	16,89	4,11	0,35
WPO	9	5,47	1,77	8	5,44	1,73	0,002
WOP	6	11,97	2,52	5	10,98	3,89	0,260
LSQ	5	10,63	3,28	4	12,26	3,86	0,467

1 Cal: caliper treatment. ImJ: ImageJ treatment. *significant statistically differences. **values not
2 calculated.

Table 2(on next page)

Descriptive statistics of all data.

Descriptive statistics of the three sorts of characters analyzed (total length and width, comprised measurements, and proportions of the measurements), including mean values (Mean), median values (Median), standard deviation values (SD), number of entries (N), and maximum and minimum values (Max-Min). All measurements are expressed in millimeters, except unscaled proportions between two measurements.

	Characters	Vector[a]	N	Mean	Median	SD	Min-Max
Total Length and Width	**TLS**	38-39	12	63.02	63.44	10.43	50.3-82.15
	TWS	-	15	63.08	58.93	11.91	48.39-94.27
Comprised measurements	**LPF**	1-4	15	8.35	8.31	1.69	4.35-10.94
	LFR	4-7	18	12.16	12.32	2.08	9.06-15.59
	LPA	7-12	12	28.88	27.36	6.45	20.54-43.80
	LVO	26-27	10	6.67	6.84	1.95	3.06-9.79
	LPAL	27-29	13	6.91	6.22	2.33	3.42-11.57
	LPT	29-30	19	11.72	11.94	2.42	6.95-17.99
	LBS	30-32	20	12.76	12.57	1.77	9.71-16.21
	LBO	32-38	13	14.16	13.38	2.12	11.13-18.28
	LMX	11-24	18	18.49	18.31	4.11	12.39-25.68
	LJU	10-14	14	12.42	12.32	3.28	4.46-17.22
	LQJ	13-18	6	11.15	10.66	2.38	8.26-14.45
	LQU	19-25	14	19.83	19.35	3.51	15.21-26.30
	LPO	6-13	17	17.54	15.72	4.12	11.51-24.59
	LSQ	20-21	11	11.71	11.08	3.07	8.24-16.57
	WPF	4-5	18	7.17	7.15	1.66	3.97-11.27
	WFR	7-8	18	10.55	10.61	1.88	7.02-13.55
	WPA	12-16	12	22.53	22.94	2.94	17.41-26.85
	SMX	11-11	15	47.85	46.35	7.63	39.24-66.10
	WVO	28-28	10	4.01	3.74	1.38	2.43-7.23
	WCO	28-34	9	7.00	6.61	1.39	5.23-9.10
	WPAL	29-35	14	18.08	18.23	2.37	15.24-21.50

	WBS	33-33	19	15.35	14.71	2.19	12.07-20.05
	WMX	10-11	16	9.80	9.84	2.24	6.48-14.27
	WJU	14-15	7	7.26	7.28	2.19	4.11-10.14
	WQJ	16-25	7	16.35	17.81	4.03	9.91-21.21
	WPO	13-14	16	5.15	5.00	1.83	2.73-9.05
	WOP	20-22	14	11.41	10.96	3.54	7.78-17.73
	CHARACTERS	**N**	**MEAN**		**MEDIAN**	**SD**	**MIN-MAX**
PROPORTIONS OF THE MEASUREMENTS	**LPF/TLS**	9	0.13		0.13	0.04	0.05-0.19
	LFR/TLS	11	0.19		0.18	0.02	0.17-0.22
	LPA/TLS	8	0.51		0.49	0.08	0.45-0.65
	LVO/TLS	8	0.11		0.12	0.03	0.06-0.15
	LPAL/TLS	10	0.11		0.11	0.03	0.06-0.17
	LPT/TLS	12	0.18		0.18	0.02	0.13-0.22
	LBS/TLS	12	0.21		0.21	0.02	0.17-0.24
	LBO/TLS	11	0.24		0.24	0.02	0.21-0.26
	LMX/TLS	11	0.29		0.28	0.06	0.17-0.38
	LJU/TLS	8	0.21		0.21	0.05	0.15-0.29
	LQJ/TLS	5	0.18		0.16	0.05	0.14-0.25
	LQU/TLS	10	0.30		0.30	0.04	0.23-0.37
	LPO/TLS	11	0.29		0.29	0.03	0.23-0.35
	LSQ/TLS	7	0.19		0.20	0.05	0.12-0.24
	WPF/TWS	13	0.12		0.12	0.02	0.08-0.15
	WFR/TWS	13	0.17		0.17	0.02	0.14-0.21
	WPA/TWS	10	0.37		0.37	0.05	0.29-0.44

SMX/TWS	12	0.75	0.76	0.06	0.67-0.86
WVO/TWS	7	0.09	0.07	0.02	0.04-0.09
WCO/TWS	7	0.11	0.12	0.02	0.09-0.13
WPAL/TWS	9	0.29	0.29	0.02	0.27-0.32
WBS/TWS	12	0.24	0.24	0.02	0.22-0.28
WMX/TWS	12	0.16	0.15	0.04	0.08-0.24
WJU/TWS	6	0.12	0.13	0.05	0.05-0.17
WQJ/TWS	7	0.29	0.30	0.08	0.16-0.37
WPO/TWS	12	0.08	0.08	0.02	0.06-0.13
WOP/TWS	11	0.18	0.17	0.04	0.13-0.23

SD: standard deviation values. N: number of entries. Max-Min: maximum and minimum values.
[a] straight line between two landmarks used to trace linear measurements (see figure 2 to visualize the landmarks).

Table 3(on next page)

PCA loadings: raw data.

Loading values of characters in the raw data matrix related to the first three principal components in PCA, comparing the Mean Value (mv) approach with the Iterative Imputation (ii) approach.

Char.	PC1 (mv)	PC2 (mv)	PC3 (mv)	PC1 (ii)	PC2 (ii)	PC3 (ii)
LPF	-0.05	0.04	0.02	-0.04	-0.05	-0.05
WPF	0.14	0.02	0.05	-0.001	0.12	0.08
LFR	0.19	-0.01	-0.09	0.02	0.14	-0.04
WFR	0.17	0.10	-0.02	0.01	0.13	-0.001
LPA	0.27	0.74	0.10	0.89	0.04	0.11
WPA	0.12	0.17	-0.01	0.22	0.16	0.06
SMX	0.66	-0.45	-0.22	0.01	0.59	-0.34
LVO	0.05	0.07	0.03	-0.02	0.11	0.01
WVO	0.04	0.03	-0.07	0.02	0.09	-0.11
WCO	0.05	0.04	-0.07	0.03	0.12	-0.08
LPAL	0.08	0.04	0.06	0.04	0.13	0.27
WPAL	0.15	0.02	-0.09	0.03	0.23	-0.05
LPT	0.17	-0.14	0.08	-0.02	0.13	0.10
LBS	0.14	-0.02	0.01	0.01	0.10	0.05
WBS	0.12	0.05	-0.07	0.02	0.19	-0.05
LBO	0.11	0.11	-0.07	0.03	0.20	0.03
LMX	0.18	-0.17	0.68	-0.18	0.16	0.38
WMX	0.09	-0.07	0.25	-0.08	0.11	0.19
LJU	0.08	0.13	0.30	-0.14	0.19	0.25
WJU	-0.01	0.02	0.10	0.01	-0.01	0.21
LQJ	0.04	-0.05	-0.04	-0.16	0.18	-0.11
WQJ	0.03	0.07	0.29	-0.11	0.17	0.42
LQU	0.18	-0.13	0.32	-0.13	0.21	0.18
LPO	0.36	0.19	-0.13	0.03	0.29	0.02
WPO	0.11	-0.04	0.05	-0.01	0.10	0.04
WOP	0.21	0.15	-0.23	0.06	0.30	-0.24
LSQ	0.07	0.19	0.11	0.16	0.02	0.43

1 Char: characters. mv: Mean Value approach. ii: Iterative Imputation approach.

Table 4(on next page)

PCA loadings: proportion data.

Loading values of characters in the proportions data matrix related to the first two principal components in PCA, comparing the Mean Value (mv) approach with the Iterative Imputation (ii) approach.

Char.	PC1 (mv)	PC2 (mv)	PC1 (ii)	PC2 (ii)
LPF/TLS	0.003	-0.13	0.11	-0.30
LFR/TLS	0.001	-0.04	0.03	-0.02
LPA/TLS	0.28	0.66	-0.13	0.67
LVO/TLS	-0.002	0.05	-0.03	-0.02
LPAL/TLS	0.08	0.02	0.07	0.12
LPT/TLS	-0.05	-0.10	-0.02	-0.01
LBS/TLS	0.03	-0.17	0.11	-0.10
LBO/TLS	-0.02	-0.04	0.01	-0.04
LMX/TLS	0.38	-0.43	0.48	-0.18
LJU/TLS	0.16	0.01	0.16	0.14
LQJ/TLS	0.06	-0.09	0.21	-0.17
LQU/TLS	0.27	-0.07	0.28	0.05
LPO/TLS	-0.16	0.13	-0.18	0.03
LSQ/TLS	0.16	0.23	0.20	0.34
WPF/TWS	0.07	0.09	-0.001	0.11
WFR/TWS	0.07	0.13	0.02	0.05
WPA/TWS	0.23	0.32	0.08	0.33
SMX/TWS	0.38	-0.12	0.33	-0.01
WVO/TWS	-0.05	-0.04	-0.04	-0.10
WCO/TWS	-0.04	0.07	-0.11	0.04
WPAL/TWS	0.04	-0.07	0.04	-0.003
WBS/TWS	0.03	-0.05	0.02	-0.03
WMX/TWS	0.35	-0.05	0.30	0.03
WJU/TWS	0.18	0.01	0.26	0.19
WQJ/TWS	0.48	-0.003	0.41	0.20
WPO/TWS	0.02	0.01	-0.01	0.07
WOP/TWS	-0.13	0.27	-0.21	0.09

1 Char: characters. mv: Mean Value approach. ii: Iterative Imputation approach.